#3

NOISE ANALYSIS OF A FINITE ELECTRON GUN IN AN INFINITE MAGNETIC FIELD

HARRISON E. ROWE

TECHNICAL REPORT 239

OCTOBER 24, 1952

RESEARCH LABORATORY OF ELECTRONICS
MASSACHUSETTS INSTITUTE OF TECHNOLOGY
CAMBRIDGE, MASSACHUSETTS

The Research Laboratory of Electronics is an interdepartmental laboratory of the Department of Electrical Engineering and the Department of Physics.

The research reported in this document was made possible in part by support extended the Massachusetts Institute of Technology, Research Laboratory of Electronics, jointly by the Army (Signal Corps), the Navy (Office of Naval Research), and the Air Force (Office of Scientific Research, Air Research and Development Command), under Signal Corps Contract DA36-039 sc-42607, Project 102B; Department of the Army Project 3-99-10-022.

MASSACHUSETTS INSTITUTE OF TECHNOLOGY

RESEARCH LABORATORY OF ELECTRONICS

Technical Report 239 October 24, 1952

NOISE ANALYSIS OF A FINITE ELECTRON GUN IN AN INFINITE MAGNETIC FIELD

Harrison E. Rowe

This report is based on a portion of a thesis submitted to the Department of Electrical Engineering, M. I. T., in partial fulfillment of the requirements for the degree of Doctor of Science, October 1952.

Abstract

A theoretical study of the noise behavior of a finite electron beam in an infinite magnetic field was made to determine the effects of the finite diameter of the beam and the transverse variations in the velocity and current density modulation on the noise behavior of an electron beam, using the method presented by Parzen for the analysis of the gun region. The presence of the higher axially-symmetric modes results in a finite standing-wave ratio of noise current in the drift space as measured by a cavity moving along the beam, as low as 10 db in some cases, as well as a behavior of partition noise which is, at least qualitatively, in agreement with that observed experimentally.

FOREWORD

The doctoral thesis from which this report is taken contained experimental work on the measurements of noise standing waves along electron beams at a frequency of approximately 3000 mc. Later work, carried out by Mr. Charles Fried, produced additional data in this field. A condensation of the results of both of these workers will be presented in a report that will be published at a later date. At this point we wish to give full credit to Dr. Rowe's ground-laying work.

L. D. Smullin

LIST OF SYMBOLS

The symbols and subscripts used in this report are defined in the following list. Most of the symbols are not defined with all of the combinations of subscripts with which they occur. All symbols for ac quantities are assumed to represent complex numbers with $\exp(j\omega t)$ time dependence implied, unless the time dependence is stated explicitly or unless mean-square values of random variables are under consideration.

a	subscript referring to the anode plane
b	beam radius
d	subscript referring to the drift space
E_n	$= \int_0^{\tau_g} K_n \, d\tau_g$, parameter in the WKB solution for the gun region
e	$= 1.6008 \times 10^{-19}$ coulombs, electron charge
f	frequency
Δf	frequency interval
f_p	plasma frequency for an electron stream of infinite transverse dimensions
f_{qn}	corrected plasma frequency for the n^{th} mode of a finite, confined beam
g	subscript referring to the gun region
I_o	total dc beam current
$I_{1/4}, I_{1/3}, I_{-3/4}, I_{-2/3}$	modified Bessel functions of the first kind, of order 1/4, 1/3, -3/4, and -2/3, respectively
i	ac current
J_o	dc current density
J_0, J_1	Bessel functions of the first kind, of order 0 and 1, respectively
j	$= \sqrt{-1}$
K	$= 1.38047 \times 10^{-23}$ joule per degree K, Boltzmann's constant
K_n^2	$= \frac{v''_{og}}{v_{og}} - \omega_{qng}^2$, parameter in the WKB solution for the gun region
K_0, K_1	modified Bessel functions of the second kind, of order 0 and 1, respectively
k	subscript referring to the cathode
m	$= 9.1066 \times 10^{-31}$ kg, mass of the electron
n	subscript indicating mode number
o	subscript indicating a dc quantity
q	ac current density modulation

$\tilde{q}$	defined by the equation $q = \tilde{q}\, J_o(Tr) \exp(-j\omega\tau)$
R	distance from the focus of a spherical electron flow
r	radius from the axis in cylindrical coordinates
T_k	cathode temperature in °K
T	radial wave number in argument of Bessel functions
t	time
V_K	cathode-to-anode voltage
V_o	dc voltage
v_o	dc velocity
v	ac velocity modulation
$\tilde{v}$	defined by the equation $v = \tilde{v}\, J_o(Tr)\, e^{-j\omega\tau}$
$v_k(r, t)$	average velocity of those electrons crossing the plane of the potential minimum between the radii r and r + dr during the time interval between t and dt
$\overline{v_k^2}$	$= \dfrac{(4-\pi)\,\eta\, K\, T_k\, \Delta f}{I_o}$, Rack noise velocity
y_n	$= v_{og}\tilde{q}_{gn}$
Z	$= \dfrac{v}{q} = \dfrac{\tilde{v}}{\tilde{q}}$, "impedance" of beam
Z_{do}	$= -\dfrac{v_{od}}{J_{od}} \cdot \dfrac{\omega_{qd}}{\omega}$, "characteristic impedance" of the beam in the drift space
z_g	distance along the axis in the gun measured from the cathode
z_d	distance along the axis in the drift space measured from the anode
γ_o	$= \dfrac{\omega}{v_o}$, phase velocity corresponding to the average beam velocity
$\Gamma(x)$	$= (x - 1)!$
δ	Dirac δ-function
Δ	symbol indicating differences
ϵ	$= 8.854 \times 10^{-12}$ farad/m, permittivity of free space
η	$= \dfrac{e}{m} = 1.7578 \times 10^{11}$ coulomb/kg, ratio of charge to mass of an electron

λ_p	plasma wavelength for an electron stream of infinite transverse dimensions
λ_{qn}	plasma wavelength for the n^{th} mode of a finite, confined beam
μ	$= \frac{R_k}{R}$, ratio of cathode sphere radius to radius from the focus of a spherical electron flow
ρ_o	$= \frac{J_o}{v_o}$, dc charge density
ρ	ac charge density
τ_g	$= \int_0^{z_g} \frac{dz_g}{v_{og}}$, dc transit time in the gun
τ_d	$\frac{z_d}{v_{od}}$, dc transit time in the drift space
ω	$= 2\pi f$, radian frequency
ω_p	$= (\eta\rho_o/\epsilon)^{1/2} = 2\pi f_p$, radian plasma frequency for an electron stream of infinite transverse dimensions
ω_{qn}	$= \omega_p \Big/ \left[1+(T_n^2/\gamma_o^2)\right]^{1/2} = 2\pi f_{qn}$, radian plasma frequency for the n^{th} mode of a finite, confined beam

I. INTRODUCTION

This report describes a theoretical investigation of noise on long electron beams at microwave frequencies. Such a study is of interest in understanding the limitations on the performance of the various types of microwave amplifiers employing electron beams.

The noise in an electron beam may be regarded as originating at the cathode, where the electrons are assumed to be emitted independently of each other, with random velocities and at random times.

At low frequencies only slow variations are of interest. Since the periods of these frequencies are long compared to the transit time of any electron through the tube, a quasi-static analysis of the situation is adequate (1, 2, 3, 4).

At high frequencies such an analysis is no longer adequate, since it may take many cycles of the frequency in question for an electron to travel through the device. Here a wave type of analysis is used. The response of the electronic system to applied sinusoidal signals is first obtained (5, 6, 7), and these results are used to describe the behavior of the device to random noise (8, 9, 10, 11, 12).

Thus A. J. Rack (9) applied F. B. Llewellyn's (5) solutions for the propagation of waves in an infinite parallel-plane electron flow to the calculation of the noise in diodes at high frequencies and further determined the appropriate input velocity modulation to be used in Llewellyn's analysis. J. R. Pierce (8), L. D. Smullin (7, 10), and D. A. Watkins (11, 12) used this type of analysis for the infinite parallel-plane diode in the gun region, matching these solutions to those of S. Ramo (6) for the lowest mode of a finite beam confined by an infinite longitudinal magnetic field in the drift space, in order to determine the noise modulation of the electron beam in the drift space.

This treatment will be referred to as the Rack-Llewellyn-Pierce analysis. It gives essentially a one-dimensional description of the problem, neglecting transverse variations of the noise modulation over the beam. Since only one mode is assumed to be present, it predicts in the drift space a standing wave of noise current having an infinite standing-wave ratio. The principal results of this analysis were first verified directly by C. C. Cutler and C. F. Quate (13), who measured the noise current modulation on the electron beam in the drift space with a re-entrant microwave cavity. They observed standing waves of noise current having, however, a finite standing-wave ratio, which was attributed to partition noise.

A great many explanations have been proposed to account for the finite minima observed in the noise standing waves on electron beams, but most noise calculations have been confined essentially to a single mode. This report attempts to evaluate the contribution of the higher modes (6) to the noise standing wave. The propagation of these different modes is determined by the geometry of the electron beam; their relative excitation is determined by the boundary conditions at the cathode.

The analysis presented in this report consequently attempts to take into account in

the noise calculations the finite size of the electron beam, both in the gun and in the drift space, and the transverse variations in the noise current and velocity modulation across the beam. Thus, these calculations lead to what might be called a two-dimensional theory rather than a one-dimensional theory. The excitation of many axially-symmetric modes, whose zeros in the drift space fall at different places, yields a small contribution to the noise current at the zeros of the fundamental mode, thus giving rise to a standing wave of noise current with finite values at the minima. A final section of the report contains a brief discussion of these results.

II. DISCUSSION OF THE MATHEMATICAL MODEL

The noise analysis of an electronic device begins with a sinusoidal analysis of the device. The sinusoidal solutions are then used to describe the noise problem by satisfying the noise boundary conditions at the cathode, or more properly, at the potential minimum.

One situation in which we are interested is that of a converging-beam Pierce gun placed in a magnetic-field-free region followed by a drift space in which the beam is focused by a uniform longitudinal magnetic field. Under ideal conditions, Brillouin flow, in which the beam radius remains constant throughout the drift space, may be attained; in practice, the flow conditions appear to be considerably more complicated.

Another case of interest is that of a parallel-beam Pierce gun followed by a drift space, with a strong uniform longitudinal magnetic field in both the gun region and the drift space. Under these conditions all transverse motion of the electrons is inhibited, and the beam has a constant radius in both the gun and the drift space.

In order to carry out ac calculations, simplifying assumptions about the dc behavior of the beam in the gun and in the drift space must be made. Consider first the Rack-Llewellyn-Pierce analysis (8, 9, 10, 11, 12, 14). This analysis utilizes the theory of the single-velocity, infinite parallel-plane diode (5, 7) for the gun region; this results in a one-dimensional theory in which all transverse variations are neglected. In the drift space the solutions of Ramo (6) for the lowest mode of a beam confined by an infinite longitudinal magnetic field are used. These are matched at the anode to the solutions for the gun region so that the ac current and velocity are continuous at the anode, yielding a standing wave in the drift space of infinite standing-wave ratio.

The infinite magnetic field model is used in the drift space because it is the simplest case to analyze, although it may be expected to apply rigorously only to a parallel-beam Pierce gun immersed in a strong magnetic field. The utilization of the infinite parallel-plane model in the gun region neglects the transverse motion of electrons, and thus is equivalent to assuming an infinite magnetic field in the direction of electron motion in the gun.

Unless the gun is a parallel-beam gun placed in the magnetic field, the cross section and the dc current density change as an electron travels from the cathode to the anode. Thus, further approximations must be made in order to apply the infinite parallel-plane analysis to the problem. This is done by replacing the actual configuration, shown in Fig. 1a, by an idealized configuration, shown in Fig. 1b.

In the idealized gun the beam is taken to be of a constant radius equal to its radius at the cathode. The infinite parallel-plane theory is applied to this finite beam by taking the gun to be a portion of an infinite parallel-plane diode. Matching the solution in the gun region to the solution for the drift space is effected by requiring that the ac current and velocity shall be continuous across the anode plane. The parallel gun immersed in

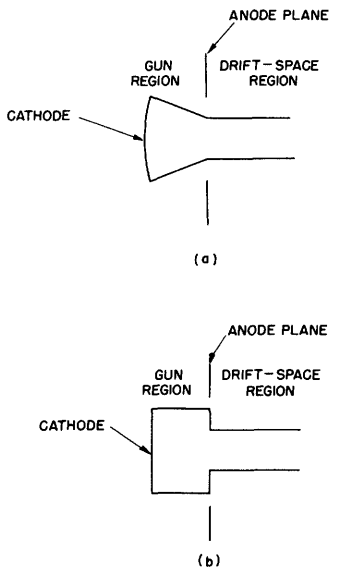

Fig. 1. Beam geometry: (a) actual; (b) idealized.

the magnetic field can be treated directly in this manner.

In addition, it is assumed that there is a thin metal electrode permeable to the electron flow in the anode plane. This electrode provides a sharp division between the gun region and the drift space for purposes of analysis and simplifies the dc solution for the beam, since the gradual transition from the gun region to the constant potential drift space caused by the fringing fields near the anode aperture is ignored.

Using this ideal gun to calculate the solution for the gun region is justified in the following manner. The greater portion of an electron's transit time in traveling from the cathode to the anode is spent near the cathode. The behavior of the ideal gun is identical with that of the actual gun near the cathode. Since the most important effects take place in this region, the calculation for the ideal gun should provide a good approximation to the actual problem.

In a space-charge-limited, single-velocity diode with zero emission velocity, the input boundary condition which must be known is the velocity modulation of the electron beam at the cathode. A real diode, in which the electrons have finite emission velocities with a Maxwellian distribution, has a potential minimum a short distance in front of the cathode. Beyond this potential minimum, however, the variation of potential is approximately the same as that of the space-charge-limited, single-velocity diode. In this region it is therefore possible to use the Llewellyn solutions for the ac behavior. However, an equivalent noise velocity modulation must be found at the plane of the potential minimum. This was done by Rack in the following manner.

Let us observe the average velocity of the electrons comprising the total dc current, I_o, of the beam crossing the potential minimum in some small interval of time dt. This average velocity, v_k, will vary with time in a random manner and will be taken as the input velocity modulation to the diode. Therefore, its mean-square value, $\overline{v_k^2}$, in the frequency range Δf must be calculated. This is called the Rack noise velocity; it is used as the input velocity at the cathode in the Llewellyn calculation.

At the cathode it is assumed that electrons are emitted with randomly distributed velocities and at random times. Therefore, in order to calculate the Rack noise velocity it would be necessary to solve the ac interaction problem in the region between the cathode and the potential minimum, using the proper boundary conditions at the cathode. Because the electron flow is a multivelocity flow in this region and electrons travel in

both directions, this is a very difficult problem to which no solution has yet been found. However, it is possible to make certain assumptions which permit an approximate solution.

If it is assumed that the transit time of electrons in the cathode-potential minimum region is very short compared to the period of the frequency being considered, it is possible to neglect transit time effects in this region and to treat fluctuations by quasi-static methods. In this manner, $\overline{v_k^2}$ was found by Rack (9) and used as the input velocity modulation for the gun region.

The results of the Rack-Llewellyn-Pierce analysis, which yield a noise-current standing wave with an infinite standing-wave ratio in the drift space, are summarized in the next section. (Meter-kilogram-second (mks) units are used throughout the report. Symbols are defined at the beginning of the report. In all formulas $\exp(j\omega t)$ time dependence is implied unless the time dependence is stated explicitly or mean-square values of random variables are under consideration.)

III. THE RACK-LLEWELLYN-PIERCE NOISE ANALYSIS (8, 10, 11, 12)

In a space-charge-limited, single-velocity diode with zero velocity of electron emission from the cathode, the velocity and current density modulation are given by

$$\tilde{v}_g = -v_{gk} \tag{1}$$

$$\tilde{q}_g = \frac{\tilde{v}_g}{Z_g} = -\frac{J_{ok}\,\omega\tau_g}{jv_{og}}\,v_{gk} \tag{2}$$

$$Z_g = \frac{v_g}{q_g} = \frac{\tilde{v}_g}{\tilde{q}_g} = j\,\frac{v_{og}}{J_{ok}\,\omega\tau_g} \tag{3}$$

The subscript g applies to the gun region; $\tilde{v}_g$ and $\tilde{q}_g$ represent the complex amplitudes of the velocity and current density modulation; v_{gk} represents the complex input velocity at the cathode; τ_g represents the dc transit time measured from the cathode. Z_g, the ratio of velocity to current density modulation, is called an "impedance," although strictly speaking, its dimensions are not those of impedance. Thus, the complex velocity and current density modulation are:

$$v_g = \tilde{v}_g \exp(-j\omega\tau_g)$$

$$q_g = \tilde{q}_g \exp(-j\omega\tau_g)$$

The dc transit time and velocity in the gun are:

$$\tau_g = \left(\frac{2v_{og}}{(\eta/\epsilon)\,J_{ok}}\right)^{1/2} \tag{4}$$

$$v_{og} = \frac{1}{2}\frac{\eta}{\epsilon}\,J_{ok}\,\tau_g^2 \tag{5}$$

In the drift space, the velocity and current density modulation of the lowest mode of a beam confined by an infinite magnetic field are, in general (6, 15),

$$\begin{aligned}\tilde{v}_d &= Z_{do}\left\{A\exp\left[-j\omega_{qd}\,\tau_d\right] + B\exp\left[+j\omega_{qd}\,\tau_d\right]\right\}\\ \tilde{q}_d &= A\exp\left[-j\omega_{qd}\,\tau_d\right] - B\exp\left[+j\omega_{qd}\,\tau_d\right]\end{aligned} \tag{6}$$

$$Z_{do} = -\frac{v_{od}}{J_{od}}\,\frac{\omega_{qd}}{\omega} \tag{7}$$

$$\tau_d = \frac{v_{od}}{z_d} \tag{8}$$

$$\omega_{qd}^2 = \frac{\omega_{pd}^2}{1 + \left(T_d^2/\gamma_{od}^2\right)} \tag{9}$$

$$\omega_{pd}^2 = \frac{\eta \rho_{od}}{\epsilon} \qquad \gamma_{od} = \frac{\omega}{v_{od}} \tag{10}$$

The subscript d applies to the drift region; ω_{pd} is the plasma frequency for an electron stream of infinite transverse dimensions; ω_{qd} is the corrected plasma frequency for the lowest mode of the finite beam. When all conducting walls are far from the beam, the radial wave number, T_d, is given by the transcendental equation

$$T_d\, b_d \frac{J_1(T_d b_d)}{J_0(T_d b_d)} = \gamma_{od}\, b_d \frac{K_1(\gamma_{od} b_d)}{K_0(\gamma_{od} b_d)} \tag{11}$$

Equations 6 and 7 are similar to the equations for a lossless transmission line, with Z_{do} analogous to the characteristic impedance of the line. The constants A and B must be chosen to match the boundary conditions at the entrance to the drift space, where $\tau_d = 0$; if the input velocity and current density modulation, v_{da} and q_{da}, are specified, v_d and q_d are determined throughout the drift space.

The output conditions of the gun will determine v_{da} and q_{da}, as given by Eqs. 1 and 2. In the actual gun, v and q must be continuous across the anode plane. In the idealized gun, however, it is not the ac current density that is required to be continuous but the total ac current, which is equal to the ac current density multiplied by the area of the beam. Thus, referring to Eqs. 1 and 2, we have

$$\begin{aligned} \tilde{v}_{da} &= \tilde{v}_{ga} \exp(-j\omega\tau_{ga}) = -v_{gk} \exp(-j\omega\tau_{ga}) \\ \tilde{q}_{da} &= \frac{J_{od}}{J_{ok}} \tilde{q}_{ga} \exp(-j\omega\tau_{ga}) = -\frac{J_{od}\, \omega\tau_{ga}}{j v_{od}} v_{gk} \exp(-j\omega\tau_{ga}) \end{aligned} \tag{12}$$

$$Z_{da} = \frac{J_{ok}}{J_{od}} Z_{ga} = j \frac{v_{od}}{J_{od}\, \omega\tau_{ga}} \tag{13}$$

Since Z_{da} is purely reactive, a perfect standing wave is established in the drift space. Solving for A and B in Eqs. 6 and 7, we find

$$\tilde{v}_d = -j\, Z_{do}\, \tilde{q}_{da} \left[1 + \left(\frac{jZ_{da}}{Z_{do}}\right)^2\right]^{1/2} \cos(\omega_{qd}\, \tau_d - \theta) \exp(-j\omega\tau_{ga}) \tag{14}$$

$$\tilde{q}_d = -\tilde{q}_{da}\left[1 + \left(\frac{jZ_{da}}{Z_{do}}\right)^2\right]^{1/2} \sin(\omega_{qd}\,\tau_d - \theta)\exp(-j\omega\tau_{ga}) \tag{15}$$

$$\cot\theta = j\frac{Z_{da}}{Z_{do}} = \frac{1}{\omega_{qd}\,\tau_{ga}} \tag{16}$$

We next substitute Eq. 12 in Eq. 15. Assuming that the ac current density is uniform across the beam, which is approximately true for the lowest mode, we multiply by the area of the beam to obtain the total ac current, and then take its mean-square value. This is the quantity measured by an ideal cavity moved along the beam. Then, using the Rack noise velocity as the input velocity modulation at the cathode,

$$\overline{v_{gk}^2} = \overline{v_k^2} = \frac{(4-\pi)\,\eta\,K\,T_k\,\Delta f}{I_o} \tag{17}$$

we finally obtain

$$\frac{\overline{i_d^2}}{2e\,I_o\,\Delta f} = \frac{(4-\pi)\,\eta\,K\,T_k}{2e}\frac{\omega^2\,\tau_{ga}^2}{v_{od}^2}\left[1 + \left(\frac{jZ_{da}}{Z_{do}}\right)^2\right]\sin^2(\omega_{qd}\,\tau_d - \theta) \tag{18}$$

$$\frac{\overline{i_d^2}}{2e\,I_o\,\Delta f} = 6.5063\times 10^6\,\frac{\omega^2\,T_k\,\tau_{ga}^2}{v_{od}^2}\left[1 + \left(\frac{jZ_{da}}{Z_{do}}\right)^2\right]\sin^2(\omega_{qd}\,\tau_d - \theta) \tag{19}$$

Equations 18 and 19 give the magnitude and phase of the noise standing wave in the drift space, according to the Rack-Llewellyn-Pierce analysis. The mean-square noise current has been normalized to pure shot noise, as in succeeding expressions.

The analysis summarized in this section suffers from several approximations. The following ones will interest us here:

a. Only the lowest mode of the drift space has been considered. The higher modes, which have longer wavelengths, will lead to a finite standing-wave ratio. In computing the excitation of this mode, the infinite parallel plane analysis of Llewellyn has been applied in an approximate manner to the gun region.

b. Since no transverse variations of velocity or current density modulation are permissible in the Llewellyn analysis, the input velocity modulation at the cathode must be constant over the cross section of the beam. This input velocity modulation is interpreted by Rack as equal to the mean-square value of the instantaneous average velocity of the electrons crossing the potential minimum. Thus, important approximations and assumptions are involved in calculating both the input conditions at the cathode and the space-charge-wave propagation in the gun region and in the drift space.

The analysis presented in the remainder of this report will undertake to construct a more realistic solution to this problem by treating the gun region as a finite,

accelerated electron stream and solving for its sinusoidal modes of propagation, matching these at the anode plane to the modes for the drift space in such a way that the ac current density and velocity are continuous. To simplify the analysis, an infinite magnetic field will be assumed to follow the electron trajectories both in the gun and in the drift space. As above, the anode plane will be assumed to consist of a conducting permeable electrode which provides a sharp transition between the gun region and the drift space.

Instead of assuming the input velocity modulation to be constant over the surface of the cathode, it is more reasonable to assume that the velocity modulation of each elementary area of the cathode is statistically independent of the velocity modulation of all other elementary areas, since it is assumed that the emission of electrons from the cathode is a completely random process. The velocity modulation of each differential area will still be given correctly by the Rack formula, where the dc current of the differential area is used in the formula. We have thus specified the boundary conditions to which we must match the sinusoidal modes of the beam.

An analysis along these lines provides what might be called a two-dimensional description of the problem, in that both the finite cross section of the beam and the statistical independence of the noise in different parts of the beam cross section are taken into account. We shall see that not only do the higher modes lead to an appreciable noise level at the minima, but their presence also gives rise to a behavior of partition noise that, at least, is in qualitative agreement with experimental evidence.

IV. THE PROPAGATION OF SPACE-CHARGE WAVES ON A FINITE ACCELERATED ELECTRON BEAM

In analyzing the sinusoidal behavior of a finite, accelerated electron stream which may vary in radius, and which is immersed in an infinite magnetic field directed along the electron trajectories, it is natural to ask whether or not the solutions for a finite, constant-radius, constant-velocity electron stream in an infinite magnetic field, as determined by Ramo (6), can be of any use. Parzen (16) has shown that under certain conditions the problem can be attacked in this manner and has given the equations for the propagation of the lowest mode in the gun. His equations are directly applicable to the higher modes by using the higher roots of the appropriate transcendental matching equation, such as Eq. 11 where conducting walls are far from the beam. A different analysis of this same problem will be given here. Its results are in no way different from those of Parzen, but it is based on a more physical approach, being analogous to the analysis of a transmission line with slowly varying parameters.

The object of the noise analysis is to determine the interaction of the noise modulation on the beam with whatever microwave structure surrounds the beam in the drift space. For example, we might wish to determine the output of a cavity used to measure the noise current modulation on the beam. Such a cavity normally is symmetric about the axis of the beam, and consequently will couple only to the axially symmetric modes of the beam. Similarly, other structures used in microwave amplifiers normally possess exact or approximate axial symmetry. Consequently, only the axial symmetric modes of the beam are considered in the present analysis. Treatment of structures that are not axially symmetric requires consideration of the beam modes with azimuthal dependence.

Figure 2 shows a sketch of the dc velocity along the beam and of the beam shape

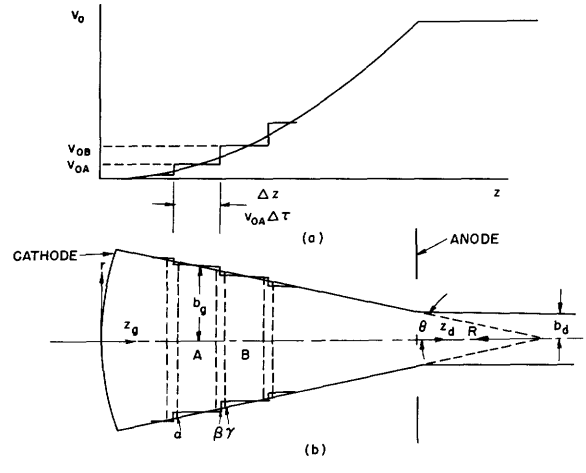

Fig. 2. Geometry of a spherically-converging-beam gun.

for a typical case. For purposes of analysis, the beam is approximated by one that consists of a series of short, cylindrical beams, each of which has a constant dc velocity, separated by abrupt changes in dc velocity and voltage, called velocity jumps.

The current density modulation for the n^{th} mode of a finite cylindrical beam confined by an infinite magnetic field is governed by the following equations (see refs. 6, 15), in which primes denote differentiation with respect to the transit time, τ_d, the independent variable:

$$\tilde{q}''_{dn} + \omega^2_{qnd}\,\tilde{q}_{dn} = 0 \tag{20}$$

$$\omega^2_{qnd} = \omega^2_{pd}/1 + \left(T^2_{nd}/\gamma^2_{od}\right); \qquad \omega^2_{pd} = \frac{\eta J_{od}}{\epsilon v_{od}}; \qquad \tau_d = \frac{z_d}{v_{od}} \tag{21}$$

$\tilde{v}_{dn}$ and $\tilde{q}_{dn}$ represent the complex amplitudes of the velocity and current density with the transverse space dependence separated out. Thus, the complex velocity and current density modulation are

$$v_{dn} = \tilde{v}_{dn}\, J_0(T_{nd}r)\, \exp(-j\omega\tau_d)$$

$$q_{dn} = \tilde{q}_{dn}\, J_0(T_{nd}r)\, \exp(-j\omega\tau_d)$$

As in Section III, ω_{pd} is the plasma frequency for an electron stream of infinite transverse dimensions; ω_{qnd} is the plasma frequency of the n^{th} mode of the finite beam. If the beam is far removed from the conducting walls, T_{nd}, the radial wave number for the n^{th} mode, is given by

$$T_{nd}\, b_d \frac{J_1(T_{nd}b_d)}{J_0(T_{nd}b_d)} = \gamma_{od}\, b_d \frac{K_1(\gamma_{od}b_d)}{K_0(\gamma_{od}b_d)} \tag{22}$$

The solutions to Eq. 20 have the form

$$\tilde{q}_{dn} = A\, \exp(-j\omega_{qnd}\, \tau_d) - B\, \exp(+j\omega_{qnd}\, \tau_d) \tag{23}$$

and the equation for the current density of the n^{th} mode is given as

$$q_{dn} = \tilde{q}_{dn}\, J_0(T_{nd}r)\, \exp(-j\omega\tau_d) \tag{24}$$

It is assumed that these solutions may be used for each of the cylindrical beams shown in the gun region in Fig. 2.

We next desire to find a general relation between the ac current and the ac velocity in an electron stream. This can be done by considering the equation of continuity and the equation defining the ac current. Let us consider a converging or diverging, accelerated beam, as illustrated in Fig. 2. Then we have the defining equation for current density and the equation of continuity:

$$q = \rho_o v + v_o \rho \tag{25}$$

$$\nabla \cdot q = -j\omega\rho$$

$$\frac{\partial q}{\partial z} - \frac{2\mu}{R_k} q = -j\omega\rho \tag{26}$$

The divergence has been taken in spherical coordinates in the last equation. Close to the cathode, the second term on the left side of Eq. 26 can be neglected; this will be done in the remainder of this section, yielding

$$\frac{\partial q}{\partial z} = -j\omega\rho \tag{27}$$

As above, we have

$$\begin{Bmatrix} q_n \\ v_n \\ \rho_n \end{Bmatrix} = \begin{Bmatrix} \tilde{q}_n \\ \tilde{v}_n \\ \tilde{\rho}_n \end{Bmatrix} J_0(T_n r) \exp(-j\omega\tau)$$

Substituting in Eqs. 25 and 27, we obtain

$$\tilde{q} = \rho_o \tilde{v} + v_o \tilde{\rho} \tag{28}$$

$$\frac{1}{v_o}\left[\frac{\partial \tilde{q}}{\partial \tau} - j\omega\tilde{q}\right] = -j\omega\tilde{\rho} \tag{29}$$

Eliminating $\tilde{\rho}$ from these equations, we finally obtain

$$\tilde{v} = \frac{v_o}{j\omega J_o}\frac{\partial \tilde{q}}{\partial \tau} = \frac{v_o}{j\omega J_o}\tilde{q}' \tag{30}$$

which is similar to an impedance relation in that it gives the relation between the amplitudes of the ac current density and ac velocity modulation. Strictly speaking, this equation is valid only when the electron flow is parallel to the z-axis. It will be approximately valid for converging or diverging flow at points not too close to the focus of the flow, but it will have a progressively greater error the closer this point is approached. Thus, the results derived here are valid only for guns in which the radius of the beam does not vary too rapidly.

Applying this relation to the current density in a drift space, as given in Eq. 23, we obtain

$$\tilde{v}_{dn} = Z_{don}\left[A \exp(-j\omega_{qnd}\,\tau_d) + B \exp(-j\omega_{qnd}\,\tau_d)\right]$$

$$Z_{don} = -\frac{v_{od}}{J_{od}}\frac{\omega_{qnd}}{\omega} \tag{31}$$

We now proceed to treat the finite, accelerated, converging, or diverging beam as a succession of finite, cylindrical, constant-velocity beams, as indicated in Fig. 2. Equations 20 and 21 specify the behavior of each cylindrical section; Eq. 30 holds as long as the gun is not too highly convergent or divergent. Since no misunderstanding is likely to arise, the subscript d will be dropped in the remainder of this section.

Using the elementary properties of derivatives, we have

$$\tilde{q}_{n\beta} = \tilde{q}_{n\alpha} + \tilde{q}'_{n\alpha}\ \Delta\tau \tag{32}$$

$$\tilde{q}'_{n\beta} = \tilde{q}'_{n\alpha} + \tilde{q}''_{n\alpha}\ \Delta\tau \tag{33}$$

The subscripts α and β refer to the corresponding reference planes of Fig. 2. Substituting Eq. 20 in Eq. 33, we obtain

$$\tilde{q}'_{n\beta} = \tilde{q}'_{n\alpha} - \omega_{qn}^2\ \tilde{q}_{n\alpha}\ \Delta\tau \tag{34}$$

Making use of Eqs. 30 and 34, we may write the velocity as

$$\tilde{v}_{n\alpha} = \frac{v_{oA}}{j\omega\ J_{oA}}\ \tilde{q}'_{n\alpha} \tag{35}$$

$$\tilde{v}_{n\beta} = \frac{v_{oA}}{j\omega\ J_{oA}}\ \tilde{q}'_{n\beta} = \frac{v_{oA}}{j\omega\ J_{oA}}\left[\tilde{q}'_{n\alpha} - \omega_{qn}^2\ \tilde{q}_{n\alpha}\ \Delta\tau\right] \tag{36}$$

The current and velocity at the input and output of a velocity jump are related by the following equations:

$$\begin{aligned} \tilde{q}_{n\gamma} &= \tilde{q}_{n\beta} \\ \tilde{v}_{n\gamma} &= \frac{v_{oA}}{v_{oB}}\ \tilde{v}_{n\beta} \end{aligned} \tag{37}$$

This can be shown either by application of the Llewellyn equations to the gap or by the conservation of energy. Thus

$$\tilde{v}_{n\gamma} = \frac{v_{oA}^2}{j\omega\ J_{oA}\ v_{oB}}\left[\tilde{q}'_{n\alpha} - \omega_{qn}^2\ \tilde{q}_{n\alpha}\ \Delta\tau\right] \tag{38}$$

Having evaluated the velocity at the two planes, it is now possible to evaluate the rate of change in velocity by subtracting $\tilde{v}_{n\alpha}$ from $\tilde{v}_{n\gamma}$ and dividing by $\Delta\tau$. Performing some algebraic manipulations, the following result is finally obtained:

$$\frac{\tilde{v}_{n\gamma} - \tilde{v}_{n\alpha}}{\Delta\tau} = \frac{\Delta\tilde{v}_n}{\Delta\tau} = -\frac{v_{oA}^2}{j\omega\ J_{oA}\ v_{oB}}\left[\tilde{q}'_{n\alpha}\ \frac{\Delta v_o}{v_{oA}\ \Delta\tau} + \omega_{qn}^2\ \tilde{q}_{n\alpha}\right] \tag{39}$$

Therefore, in the limit as $\Delta\tau \to 0$,

$$\tilde{v}'_n = -\frac{v_o}{j\omega J_o}\left[\frac{v'_o}{v_o}\tilde{q}'_n + \omega_{qn}^2 \tilde{q}_n\right] \tag{40}$$

However, subject to the assumptions stated above, Eq. 30 is good, in general, for $\tilde{v}_n$, and when differentiated, it yields another expression for $\tilde{v}'_n$:

$$\tilde{v}'_n = \frac{v_o}{j\omega J_o}\left[\tilde{q}''_n + \frac{v'_o}{v_o}\tilde{q}'_n\right] \tag{41}$$

In performing this differentiation it has again been assumed that the gun is only slightly convergent or divergent so that derivatives of J_o may be neglected. Similar assumptions were made in deriving Eq. 30. Equations 40 and 41 yield the desired differential equation for $\tilde{q}_n$ in the gun region:

$$\tilde{q}''_{gn} + 2\frac{v'_{og}}{v_{og}}\tilde{q}'_{gn} + \omega_{qng}^2 \tilde{q}_{gn} = 0 \tag{42}$$

$$\tau_g = \int_0^{z_g} \frac{dz_g}{v_{og}}; \qquad \omega_{qng}^2 = \frac{\omega_{pg}^2}{1 + \left(T_{ng}^2/\gamma_{og}^2\right)}; \qquad \omega_{pg}^2 = \frac{\eta J_{og}}{\epsilon v_{og}} \tag{43}$$

$$T_{ng} b_g \frac{J_1(T_{ng} b_g)}{J_0(T_{ng} b_g)} = \gamma_{og} b_g \frac{K_1(\gamma_{og} b_g)}{K_0(\gamma_{og} b_g)} \tag{44}$$

This is the equation obtained by Parzen. Together with Eq. 30, which gives $\tilde{v}_n$ in terms of $\tilde{q}_n$, it gives the complete behavior of the space-charge waves in the gun region.

It must be emphasized once again that this equation is the result of several approximations and must be expected to apply rigorously only when the gun is not too highly convergent or divergent. It is not clear what types of error arise when these approximations are no longer valid. However, this analysis will be applied to both parallel- and converging-beam Pierce guns because no more rigorous analysis is available at present.

V. SOLUTIONS IN THE FINITE GUN AND IN THE DRIFT SPACE

From the results of Section IV, it is seen that Eqs. 42 and 30 describe approximately the propagation of space-charge waves in the gun region:

$$\tilde{q}''_{gn} + 2\frac{v'_{og}}{v_{og}}\tilde{q}'_{gn} + \omega^2_{qng}\,\tilde{q}_{gn} = 0 \tag{42}$$

$$\tilde{v}_{gn} = \frac{v_{og}}{j\omega J_{og}}\tilde{q}'_{gn} \tag{30}$$

In the drift space v'_o is zero; and the solutions to Eq. 42 are the ordinary Ramo waves, as given in Eqs. 23, 24, and 31. These equations are applicable to any gun as long as the beam radius does not change too rapidly. They will be applied in this report to converging- and parallel-beam Pierce guns having the geometry illustrated in Fig. 2b.

Parzen (16) presented an approximate solution to Eq. 42 based on the Wentzel-Kramers-Brillouin (WKB) method (see Appendix A and refs. 17 and 18). If we make the following transformation:

$$\tilde{q}_{gn} = \frac{y_n}{v_{og}}$$

then Eq. 42 becomes

$$y''_n - K_n^2\, y_n = 0 \tag{45}$$

$$K_n^2 = \frac{v''_{og}}{v_{og}} - \omega^2_{qng} \tag{46}$$

This equation has no first derivative and it is suitable for the application of the WKB technique. Taking account of the fact that K_n^2 has a zero at the origin, $\tau_g = 0$, and assuming that $K_n^2 > 0$, the WKB solution of Eq. 45 is

$$y_n = \left[\frac{E_n}{K_n}\right]^{1/2} I_{1/3}^{1/4}(E_n) \tag{47}$$

$$E_n = \int_0^{\tau_g} K_n\, d\tau_g \tag{48}$$

Here I represents a modified Bessel function of the first kind. The order of this Bessel function is 1/4 or 1/3, applying, respectively, to the parallel-beam gun and the converging-beam gun. This difference in order is caused by the fact that while K_n^2

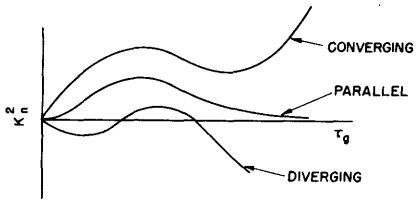

Fig. 3. K_n^2 versus τ_g for converging-beam, parallel-beam, and diverging-beam guns.

has a second-order zero at the origin for a parallel-beam gun, it has only a first-order zero for a converging- or diverging-beam gun. Although solutions of negative order also satisfy the differential equation, these solutions have been discarded because the velocity modulation at the cathode in these solutions goes to infinity. In the solutions of positive order, the velocity modulation at the cathode approaches a constant value; these solutions may therefore be used in matching the appropriate boundary conditions at the cathode.

Equations 47 and 48 are correct solutions for the gun region only when K_n^2 remains positive throughout the gun region, which it does for converging- and parallel-beam guns. For diverging-beam guns, K_n^2 becomes negative in certain regions, making K_n imaginary. Figure 3 shows the typical behavior of K_n^2 for converging-, parallel-, and diverging-beam guns.

As shown above, the proper solutions for the converging and the parallel cases are the modified Bessel functions, $I_{+1/3}$ and $I_{+1/4}$, respectively. In the diverging case the problem is slightly more complicated. In the regions where K_n becomes imaginary, the Bessel functions $J_{\pm 1/3}$ must be used; where K_n is real, the modified Bessel functions $I_{\pm 1/3}$ are used, as in the converging case. The solutions in the different regions must then be properly matched at the boundaries. Diverging-beam guns are not considered further in this report.

We have, therefore, the following solutions for the gun region:

Parallel-Beam Gun

$$\tilde{q}_{gn} = \frac{1}{v_{og}} \left[\frac{E_n}{K_n}\right]^{1/2} I_{1/4}(E_n) \tag{49}$$

$$\tilde{v}_{gn} = Z_{gn}\, \tilde{q}_{gn} \tag{50}$$

$$Z_{gn} = \frac{v_{og}}{j\omega J_{og}} \left[K_n \frac{I_{-3/4}(E_n)}{I_{+1/4}(E_n)} + \frac{1}{4}\frac{K_n}{E_n} - \frac{1}{2}\frac{K_n'}{K_n} - \frac{v_{og}'}{v_{og}}\right] \tag{51}$$

As $\tau_g \to 0$

$$\tilde{q}_{gn} \to \frac{\left[\frac{\epsilon}{\eta}\right]^{3/4}}{2^{1/8}\,\Gamma(5/4)\, J_{ok}^{3/4}} \frac{1}{\left[\frac{T_{nk}}{\omega}\right]^{1/4}} \frac{1}{\tau} = 1.912 \times 10^{-17} \frac{1}{J_{ok}^{3/4}} \left[\frac{T_{nk}}{\omega}\right]^{1/4} \frac{1}{\tau} \tag{52}$$

$$\tilde{v}_{gn} \to j \frac{1}{2.2^{1/8}\,\Gamma(5/4)} \left[\frac{\eta}{\epsilon}\right]^{1/4} \frac{T_{nk}^{1/4}}{J_{ok}^{3/4}\,\omega^{5/4}} = j\,1.899 \times 10^{5} \frac{T_{nk}^{1/4}}{J_{ok}^{3/4}\,\omega^{5/4}} \tag{53}$$

$$T_n \to T_{nk} \qquad J_0(T_{nk} b_k) = 0 \tag{54}$$

Spherically Converging Beam Gun

$$\tilde{q}_{gn} = \frac{1}{v_{og}} \left[\frac{E_n}{K_n}\right]^{1/2} I_{1/3}(E_n) \tag{55}$$

$$\tilde{v}_{gn} = Z_{gn}\,\tilde{q}_{gn} \tag{56}$$

$$Z_{gn} = \frac{v_{og}}{j\omega\, J_{og}} \left[K_n \frac{I_{-2/3}(E_n)}{I_{+1/3}(E_n)} + \frac{1}{6}\frac{K_n}{E_n} - \frac{1}{2}\frac{K_n'}{K_n} - \frac{v_{og}'}{v_{og}}\right] \tag{57}$$

As $\tau_g \to 0$

$$\tilde{q}_{gn} \to \frac{2.2^{2/3}}{3^{5/6}\,\Gamma(4/3)} \left[\frac{\epsilon}{\eta}\right]^{5/6} \frac{1}{R_k^{1/6}\,J_{ok}^{5/6}} \frac{1}{\tau} = 3.735 \times 10^{-19} \frac{1}{R_k^{1/6}\,J_{ok}^{5/6}} \frac{1}{\tau} \tag{58}$$

$$\tilde{v}_{gn} \to j \frac{2^{2/3}}{3^{5/6}\,\Gamma(4/3)} \left[\frac{\eta}{\epsilon}\right]^{1/6} \frac{1}{R_k^{1/6}\,J_{ok}^{5/6}\,\omega} = j\,3.705 \times 10^{3} \frac{1}{R_k^{1/6}\,J_{ok}^{5/6}\,\omega} \tag{59}$$

$$T_n \to T_{nk} \qquad J_0(T_{nk} b_k) = 0 \tag{60}$$

In these formulas, K_n and E_n are given by Eqs. 46 and 48, respectively.

These solutions must be evaluated by numerical and graphical methods; they are based on the dc properties of the gun. The potential distribution and the transit time are given for the parallel gun by simple formulas; the spherical space-charge-limited flow has been worked out by Langmuir and Blodgett (19). The formulas and tables of functions necessary for evaluating the various parameters are given in Appendices B, C, D, and E.

We must next match these solutions for the gun to the Ramo solutions for the drift space by matching velocity and current density or, equivalently, impedance, across the anode plane. The Ramo solutions, as stated in Eqs. 6-10 and in Eqs. 23, 24, and 31 are

$$\tilde{q}_{dn} = A \exp(-j\omega_{qnd}\,\tau_d) - B \exp(+j\omega_{qnd}\,\tau_d) \tag{61}$$

$$\tilde{v}_{dn} = Z_{don}\left[A \exp(-j\omega_{qnd}\,\tau_d) + B \exp(+j\omega_{qnd}\,\tau_d)\right] \tag{62}$$

$$\tau_d = \frac{z_d}{v_{od}} \tag{63}$$

$$Z_{don} = -\frac{v_{od}}{J_{od}} \frac{\omega_{qnd}}{\omega} \tag{64}$$

Since $\tilde{v}_n$ and $\tilde{q}_n$ are 90° out of phase in the gun, a perfect standing wave is established in the drift space for each mode. Thus, as with Eq. 15, the continuity of v_n and q_n at the anode yields

$$\tilde{q}_{dn} = -\tilde{q}_{gna} \left[1 + \left(\frac{jZ_{gna}}{Z_{don}} \right)^2 \right]^{1/2} \sin(\omega_{qnd} \tau_d - \theta_n) \exp(-j\omega\tau_{ga}) \tag{65}$$

$$\cot \theta_n = \frac{jZ_{gna}}{Z_{don}} \tag{66}$$

It is not the ac current density but the total ac current which is of interest. This is the quantity that would be measured by an ideal cavity, with unity coupling coefficient, moving along the beam in the drift space. The total ac current is obtained by integrating the current density across the cross section of the beam:

$$\begin{aligned} i_{dn} &= \int_0^{b_d} q_{dn} \cdot 2\pi r \, dr = 2\pi \, \tilde{q}_{dn} \exp(-j\omega \tau_d) \int_0^{b_d} r \, J_0(T_{nd} r) \, dr \\ i_{dn} &= \pi \, b_d^2 \cdot \frac{2}{T_{nd} b_d} J_1(T_{nd} b_d) \, \tilde{q}_{dn} \exp(-j\omega\tau_d) \end{aligned} \tag{67}$$

We have now obtained approximate solutions for the propagation of space-charge waves in the gun and in the drift space; only the axially-symmetric solutions have been considered, since only these solutions couple to the cavity and contribute to the total ac current in the beam. We must next consider the problem of matching the statistical boundary conditions at the cathode, or strictly speaking, at the potential minimum, with these sinusoidal solutions.

VI. THE STATISTICAL PROBLEM: MATCHING AT THE CATHODE

In general, the velocity and current density modulation will be expressed as a summation over all of the modes of the beam:

$$\begin{matrix} v \\ q \end{matrix}(r, \tau) \exp(j\omega t) = \sum_n A_n \begin{matrix} v_n \\ q_n \end{matrix}(r, \tau) \exp(j\omega t)$$

$$= \sum_n A_n \begin{matrix} \tilde{v}_n \\ \tilde{q}_n \end{matrix}(\tau) J_0(T_n r) \exp\left[j\omega(t-\tau)\right] \tag{68}$$

Here, for reasons discussed before, only the axially-symmetric modes are considered. Equation 68 applies either to the gun region or to the drift space, using the appropriate solutions for v_n and q_n as given in Eqs. 49-60 and Eqs. 61-67.

We have thus far considered only sinusoidal time dependence. We now wish to include arbitrary variations with time, in order to apply this analysis to the noise problem. If we consider the fluctuations in a narrow-frequency band $\Delta\omega$ about the center frequency ω, Eq. 68 may be rewritten for arbitrary time dependence as

$$\begin{matrix} v \\ q \end{matrix}(r, \tau, t) = \sum_n B_n(t-\tau) \begin{matrix} \tilde{v}_n \\ \tilde{q}_n \end{matrix}(\tau) J_0(T_n r) \tag{69}$$

The restriction to a narrow-frequency band is necessary because $\tilde{v}_n(\tau)$ and $\tilde{q}_n(\tau)$ are slowly varying functions of frequency. However, the cavity used to measure the noise current in the drift space responds only to a narrow band of frequencies, so that this restriction does not prove inconvenient.

As mentioned in Section V, the quantities of interest are not the ac velocity and current density, but rather the average ac velocity across the beam and the total ac current modulation, which is the quantity measured by an ideal cavity. If in Eq. 69 random variations are being considered, the average ac velocity and the total ac current will also be random variables, and we shall be interested in their mean-square values. These are given by the following expressions:

$$\overline{(\bar{v}^r)^2} = \overline{\left[\frac{\int_0^b v(r, \tau, t) \cdot 2\pi r \, dr}{\pi b^2}\right]^2} = \overline{\left[\sum_n B_n(t-\tau) \tilde{v}_n(\tau) \frac{2}{T_n b} J_1(T_n b)\right]^2} \tag{70}$$

$$\overline{i^2} = \overline{\left[\int_0^b q(r, \tau, t) \cdot 2\pi r \, dr\right]^2} = \overline{\left[\pi b^2 \sum_n B_n(t-\tau) \tilde{q}_n(\tau) \frac{2}{T_n b} J_1(T_n b)\right]^2} \tag{71}$$

In evaluating these expressions it will be necessary to evaluate quantities of the form $\overline{B_m B_n}$ and $\overline{B_n^2}$. The statistical properties of the B_n must be obtained by matching the solutions for the gun to the boundary conditions at the cathode, which must specify the velocity modulation there.

The Rack noise velocity is given by

$$\overline{v_k^2} = \frac{(4-\pi)\,\eta\,K\,T_k\,\Delta f}{I_{dc}} \tag{72}$$

This equation gives the mean-square value of the fluctuations in the average velocity of the electrons comprising the dc current, I_{dc}, crossing the potential minimum in front of a space-charge-limited cathode.

As indicated above, the boundary conditions at the cathode will be specified in the following manner. The cathode will be divided into elementary areas, each having an elementary dc current associated with it. Equation 72 will be assumed to give the correct mean-square velocity modulation for each elementary area; it will be further assumed that the velocity modulations of all of the elementary areas are statistically independent. Because only the axially-symmetric modes are of interest here, the elementary area will consist of the region lying between the radii r and r+ dr. As this elementary area approaches zero, the dc current approaches zero, and the mean-square velocity modulation given by Eq. 72 approaches infinity. Thus, the boundary conditions on the velocity modulation at the cathode may be specified by

$$\overline{v_k(r,t)\,v_k(s,t)} = \frac{(4-\pi)\,\eta\,K\,T_k\,\Delta f\,b_k^2}{I_o\,2r}\,\delta(r-s) \tag{73}$$

Here, r and s are two different radii, I_o is the total dc current emitted from the cathode, b_k is the cathode radius, and δ denotes the Dirac δ-function. Equation 73 states that the crosscorrelation function of the noise velocities of two different areas of the cathode is zero, while the mean-square noise velocity from a single area of the cathode is given by Rack's formula (Eq. 72).

To match the series solution for the gun region to the boundary conditions at the cathode, we set $\tau = 0$ in Eq. 69, obtaining

$$v_{gk}(r,t) = \sum_n B_n(t)\,\tilde{v}_{gn}(0)\,J_0(T_{nk}r)$$
$$J_0(T_{nk}b_k) = 0 \tag{74}$$

where $\tilde{v}_{gn}(0)$ is given by Eqs. 53 and 59 for the parallel and the spherical cases, respectively. Thus

$$v_{gk}(r,t) = \sum_n C_n(t)\,J_0(T_{nk}r), \qquad J_0(T_{nk}b_k) = 0 \tag{75}$$

$$C_n(t) = B_n(t)\, \tilde{v}_{gn}(0) \tag{76}$$

From the theory of Fourier-Bessel series (20), we have

$$C_n(t) = \frac{2}{b_k^2\, J_1^2(T_{nk} b_k)} \int_0^{b_k} r\, v_{gk}(r,t)\, J_0(T_{nk} r)\, dr \tag{77}$$

Therefore

$$\overline{C_m(t)\, C_n(t)} = \frac{4}{b_k^4\, J_1^2(T_{mk} b_k)\, J_1^2(T_{nk} b_k)} \int_0^{b_k} r\, J_0(T_{mk} r)\, dr$$

$$\cdot \int_0^{b_k} \overline{v_{gk}(r,t)\, v_{gk}(s,t)}\, s\, J_0(T_{nk} s)\, ds \tag{78}$$

Using Eq. 73, we obtain

$$\overline{C_m(t)\, C_n(t)} = \frac{(4-\pi)\, \eta K T_k\, \Delta f}{I_o} \frac{2}{b_k^2\, J_1^2(T_{mk} b_k)\, J_1^2(T_{nk} b_k)}$$

$$\cdot \int_0^{b_k} J_0(T_{mk} r)\, dr \int_0^{b_k} \delta(r-s)\, s\, J_0(T_{nk} s)\, ds \tag{79}$$

$$\overline{C_m(t)\, C_n(t)} = \frac{(4-\pi)\, \eta K T_k\, \Delta f}{I_o} \frac{2}{b_k^2\, J_1^2(T_{mk} b_k)\, J_1^2(T_{nk} b_k)}$$

$$\cdot \int_0^{b_k} r\, J_0(T_{mk} r)\, J_0(T_{nk} r)\, dr \tag{80}$$

By the orthogonality relations for Bessel functions, the integral in Eq. 80 is zero if $m \neq n$. Therefore we have

$$\overline{C_m(t) \cdot C_n(t)} = 0, \quad m \neq n \tag{81}$$

When $m = n$, we have

$$\overline{C_n^2(t)} = \frac{(4-\pi)\, \eta K T_k\, \Delta f}{I_o} \frac{1}{J_1^2(T_{nk} b_k)} \tag{82}$$

Having thus determined the C_n, we can determine the B_n from Eqs. 76, 53, and 59; and we can now evaluate Eqs. 70 and 71, obtaining the mean-square values of the average ac velocity across the beam and the total ac current modulation on the beam.

We see from Eq. 81 that the various modes are statistically independent. Therefore,

all of the cross-terms in the expansions given in Eqs. 70 and 71 vanish, leaving only the summation of the mean-square amplitudes of each mode averaged over the cross section.

These results are very different from those that would have been obtained if the input velocity modulation at the cathode had been assumed to be constant over the cross section of the beam.

At the cathode, the Rack formula (Eq. 72) must give the mean-square value of the average ac velocity across the cathode; Eq. 70, with Eqs. 81 and 82, must yield an equivalent answer if the mode description presented above is correct. Thus

$$\frac{(4-\pi)\,\eta\,K\,T_k\,\Delta f}{I_o} = \sum_n \overline{C_n^2(t)}\,\frac{4}{(T_{nk}b_k)^2}\,J_1^2(T_{nk}b_k)$$

$$\frac{(4-\pi)\,\eta\,K\,T_k\,\Delta f}{I_o} = \frac{(4-\pi)\,\eta\,K\,T_k\,\Delta f}{I_o}\sum_{n=1}^{\infty}\frac{4}{(T_{nk}b_k)^2} \tag{83}$$

$$0.25 = \sum_{n=1}^{\infty}\frac{1}{(T_{nk}b_k)^2} \qquad J_0(T_{nk}b_k) = 0 \tag{84}$$

Equation 84 is a known identity (21).

A summary of the results derived here is next presented.

VII. SUMMARY OF RESULTS FOR PARALLEL AND SPHERICALLY CONVERGING BEAM GUNS

Parallel-Beam Gun

$$\frac{\overline{i_d^2}}{2e\, I_o\, \Delta f} = 8 \cdot 2^{1/4}\, \Gamma^2(5/4)\,(4-\pi)\,\frac{\eta K}{e}\left[\frac{\epsilon}{\eta}\right]^{1/2} \frac{T_k\, J_{ok}^{3/2}\, \omega^{5/2}}{I_o^2}$$

$$\cdot \left[\pi b_d^2\right]^2 \sum_{n=1}^{\infty} \frac{J_1^2(T_{nd} b_d)}{T_{nk}^{1/2}(T_{nd} b_d)^2\, J_1^2(T_{nk} b_k)} \cdot \tilde{q}_{gna}^2$$

$$\cdot \left[1 + \left(\frac{j\, Z_{gna}}{Z_{don}}\right)^2\right] \sin^2(\omega_{qnd}\, \tau_d - \theta_n)$$

$$= 7.219 \times 10^{-4}\, \frac{T_k\, J_{ok}^{3/2}\, \omega^{5/2}}{I_o^2} \left[\pi b_d^2\right]^2 \sum_{n=1}^{\infty} \frac{J_1^2(T_{nd} b_d)}{T_{nk}^{1/2}(T_{nd} b_d)^2\, J_1^2(T_{nk} b_k)}$$

$$\cdot \tilde{q}_{gna}^2 \left[1 + \left(\frac{j\, Z_{gna}}{Z_{don}}\right)^2\right] \sin^2(\omega_{qnd}\, \tau_d - \theta_n) \tag{85}$$

$$\tilde{q}_{gn} = \frac{1}{v_{og}} \left[\frac{E_n}{K_n}\right]^{1/2} I_{1/4}(E_n) \tag{86}$$

$$Z_{gn} = \frac{v_{og}}{j\omega\, J_{og}} \left[K_n \frac{I_{-3/4}(E_n)}{I_{+1/4}(E_n)} + \frac{1}{4}\frac{K_n}{E_n} - \frac{1}{2}\frac{K_n'}{K_n} - \frac{v_{og}'}{v_{og}}\right] \tag{87}$$

$$K_n^2 = 2\left[\frac{1}{2}\,\frac{\eta}{\epsilon}\right]^2 \left[\frac{J_{ok}}{\omega}\right]^2 \frac{T_{ng}^2\, \tau_g^2}{1 + \left[\frac{1}{2}\,\frac{\eta}{\epsilon}\right]^2 \left[\frac{J_{ok}}{\omega}\right]^2 T_{ng}^2\, \tau_g^4}$$

$$= 1.972 \times 10^{44} \left[\frac{J_{ok}}{\omega}\right]^2 \frac{T_{ng}^2\, \tau_g^2}{1 + 0.9860 \times 10^{44} \left[\frac{J_{ok}}{\omega}\right]^2 T_{ng}^2\, \tau_g^4} \tag{88}$$

$$v_{og} = \frac{1}{2}\,\frac{\eta}{\epsilon} J_{ok}\, \tau_g^2 = 9.930 \times 10^{21}\, J_{ok}\, \tau_g^2 \tag{89}$$

$$\frac{v'_{og}}{v_{og}} = \frac{2}{\tau_g} \tag{90}$$

$$V_{og} = \frac{1}{8}\frac{\eta}{\epsilon^2} J_{ok}^2 \tau_g^4 = 2.804 \times 10^{32} J_{ok}^2 \tau_g^4 \tag{91}$$

Spherically Converging Beam Gun

$$\frac{\overline{i_d^2}}{2e I_o \Delta f} = \frac{3^{5/3}\,\Gamma^2(4/3)(4-\pi)}{2^{1/3}} \frac{\eta K}{e}\left[\frac{\epsilon}{\eta}\right]^{1/3} \frac{T_k R_k^{1/3} J_{ok}^{5/3} \omega^2}{I_o^2}$$

$$\cdot \left[\pi b_d^2\right]^2 \sum_{n=1}^{\infty} \frac{J_1^2(T_{nd} b_d)}{(T_{nd} b_d)^2 J_1^2(T_{nk} b_k)} \tilde{q}_{gna}^2$$

$$\cdot \left[1 + \left(\frac{j Z_{gna}}{Z_{don}}\right)^2\right] \sin^2(\omega_{qnd} \tau_d - \theta_n)$$

$$= 1.898 \frac{T_k R_k^{1/3} J_{ok}^{5/3} \omega^2}{I_o^2} \left[\pi b_d^2\right]^2 \sum_{n=1}^{\infty} \frac{J_1^2(T_{nd} b_d)}{(T_{nd} b_d)^2 J_1^2(T_{nk} b_k)}$$

$$\cdot \tilde{q}_{gna}^2 \left[1 + \left(\frac{j Z_{gna}}{Z_{don}}\right)^2\right] \sin^2(\omega_{qnd} \tau_d - \theta_n) \tag{92}$$

$$\tilde{q}_{gn} = \frac{1}{v_{og}}\left[\frac{E_n}{K_n}\right]^2 I_{1/3}(E_n) \tag{93}$$

$$Z_{gn} = \frac{v_{og}}{j\omega J_{og}}\left[K_n \frac{I_{-2/3}(E_n)}{I_{+1/3}(E_n)} + \frac{1}{6}\frac{K_n}{E_n} - \frac{1}{2}\frac{K'_n}{K_n} - \frac{v'_{og}}{v_{og}}\right] \tag{94}$$

$$K_n^2 = \frac{v''_{og}}{v_{og}} - \omega_{qng}^2 \tag{95}$$

The spherical formulas and functions that are necessary for performing these calculations are given in Appendices B, C, and D.

$$Z_{don} = -\frac{v_{od}}{J_{od}} \frac{\omega_{qnd}}{\omega} \tag{96}$$

$$\tau_d = \frac{z_d}{v_{od}} \tag{97}$$

$$\cot \theta_n = \frac{j Z_{gna}}{Z_{don}} \tag{98}$$

$$E_n = \int_0^{\tau_g} K_n d \tau_g \tag{99}$$

The following equation holds true both in the gun and in the drift space:

$$(T_n b) \frac{J_1(T_n b)}{J_0(T_n b)} = (\gamma_o b) \frac{K_1(\gamma_o b)}{K_0(\gamma_o b)} \tag{100}$$

If we assume the drift tube walls are far from the beam,

$$\omega_{qn}^2 = \frac{\omega_p^2}{1 + \left(T_n^2/\gamma_o^2\right)} \qquad \omega_p^2 = \frac{\eta}{\epsilon} \frac{J_o}{v_o} \tag{101}$$

(The primes denote differentiation with respect to τ_g.)

Tables of the combinations of Bessel functions appearing in Eq. 100 are given in Appendix D.

VIII. SCALING LAWS

By the application of dimensional analysis to the equations given in Section VII, the scaling laws summarized in Table I can be derived. The three lines in this table represent three different ways in which the problem may be scaled. If V_K, I_o, b, and f are multiplied by the indicated factors, $\overline{i_d^2}$ and f_q will scale as indicated.

Note that scaling the beam radius, b, is not equivalent to scaling all dimensions of the problem, but only the radial dimensions (such as the cathode radius or the beam radius in the drift space). The axial dimensions will, in general, scale differently.

Table I

Scaling Laws for Parallel and Spherical Guns

	V_K	I_o	b	f	$\overline{i_d^2}$	f_q
1.	1	a	1	1	1	$a^{1/2}$
2.	b^2	1	b	1	b	$b^{-3/2}$
3.	1	1	c^{-1}	c	1	c

Table II

Electron Gun Parameters

Gun	Type	Angle of Convergence	$\frac{R_k}{R_a}$	b_k (meters $\times 10^{-4}$)	b_d (meters $\times 10^{-4}$)	Perveance ($av^{-3/2} \times 10^{-7}$)
A	converging	7.3°	2.2	16.76	7.620	1.131
B	converging	3.3°	1.5	11.43	7.620	1.131
C	parallel	0°	1.0	7.620	7.620	1.131
D	parallel	0°	1.0	7.620	7.620	0.5655
E	parallel	0°	1.0	7.620	7.620	2.262
F	parallel	0°	1.0	3.810	3.810	1.131
G	parallel	0°	1.0	15.24	15.24	1.131

For all cases: f = 3000 mc, T_k = 1000 K.

IX. NOISE BEHAVIOR OF SPECIFIC ELECTRON GUNS

In order to determine the effect of the gun parameters on the noise standing wave in the drift space, the calculations summarized above were carried out for seven different guns. The important parameters of these guns are summarized in Table II.

The parameters of gun A have been selected to agree approximately with those of gun 1040, on which noise measurements have been performed (22), to permit a comparison between experiment and theory.

Guns A, B, and C have the same perveance and beam radius in the drift space but have different angles of convergence in the gun region. Guns C, D, and E are parallel guns of the same beam radius but of different perveance. Guns C, F, and G are parallel guns of the same perveance but of different beam radius. Thus, the calculations carried out for these guns permit the investigation of the effects of varying the angle of convergence of the gun, the perveance, and the radius of the beam on the noise standing wave observed in the drift space.

Calculations were made for guns A, B, and C at 1000 volts, 1250 volts, and 1500 volts; calculations were made for guns D, E, F, and G at 1250 volts only. In addition, the noise for gun A was evaluated at 500 volts. Only the first four modes have been considered in these calculations.

The maxima and the minima of the noise standing wave patterns for these different cases have been plotted in Figs. 4-7; the remainder of the standing-wave pattern has been sketched in each case. Figure 4a, b, c gives the noise standing wave curves for guns A, B, and C at V_K = 1000 volts, 1250 volts, and 1500 volts, respectively, showing the effect of varying the angle of convergence of the gun on the noise standing wave. Figure 5 gives the noise standing wave for gun A at V_K = 500 volts. Figure 6 shows the standing-wave patterns for guns C, D, and E at V_K = 1250 volts, illustrating the effect of varying the perveance of the gun. Note that the three curves are identical and are separated by 3 db; this is one illustration of the scaling laws given in Section VIII. Figure 7 gives the standing-wave curves for guns C, F, and G at V_K = 1250 volts, showing the effect of varying the beam radius.

The following general observations may be made on these theoretical results:

a. The presence of the higher modes results in a finite minimum of the standing-wave pattern, with a standing-wave ratio as low as 10 db in some cases. In general, the different minima have different levels.

b. Neglecting the first minimum, we find that a converging beam gun has a lower standing-wave ratio than a parallel beam gun, assuming that the total beam current and the radius of the beam in the drift space are the same. The first minimum, however, is much deeper than that for a parallel gun. In addition, the level of the noise maxima is lower for a converging gun than for a parallel gun.

c. Varying the total beam current, while keeping the beam voltage, beam radius, and cathode radius constant, leaves the absolute level of the noise maxima and minima

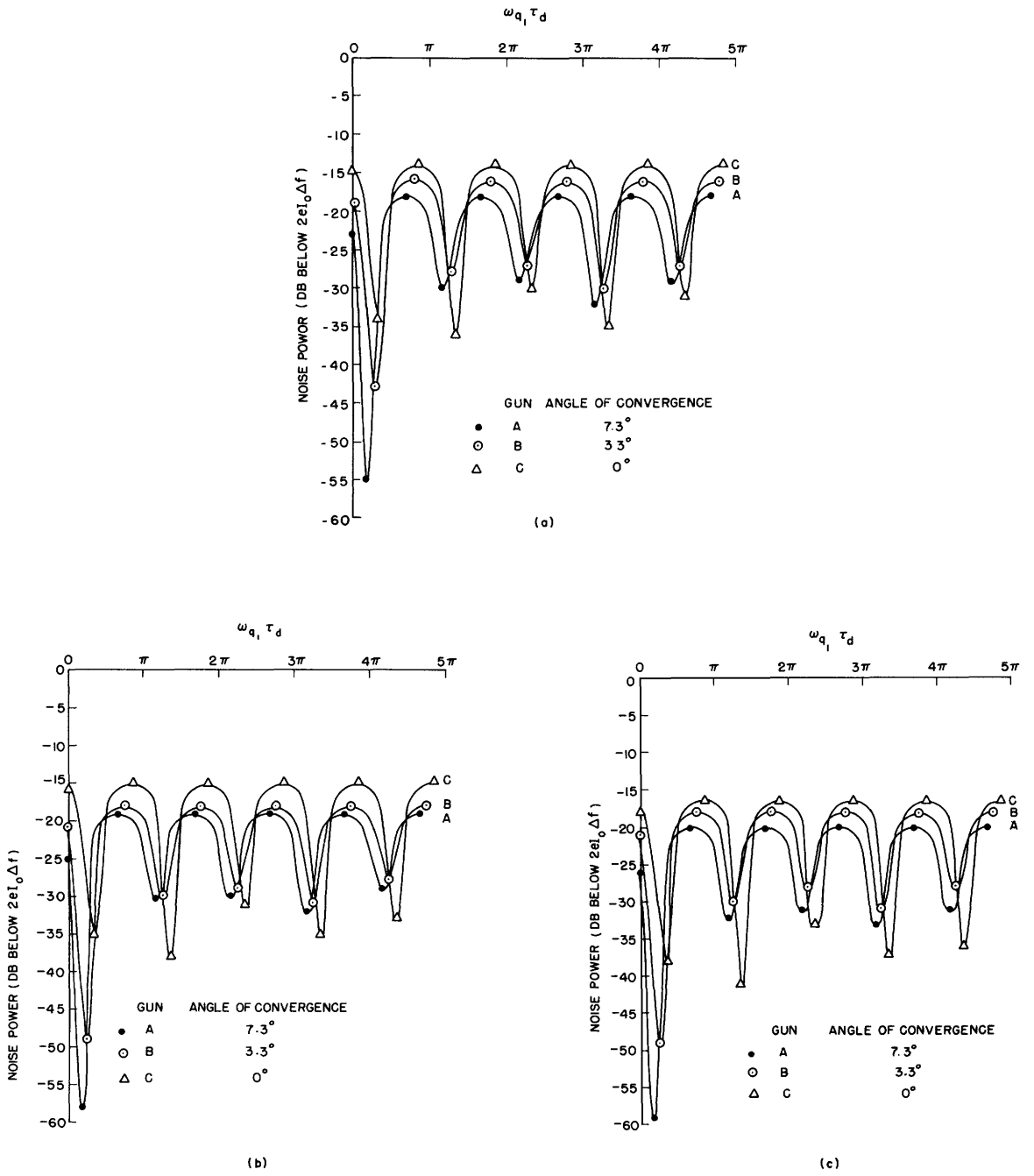

Fig. 4. Effect of the angle of convergence of the gun on the noise standing wave; (a) V_K = 1000 volts, I_o = 3.575 ma, $b_d = 7.620 \times 10^{-4}$ m, $\omega_{q1} = 0.7156 \times 10^9$; (b) V_K = 1250 volts, I_o = 5.000 ma, $b_d = 7.260 \times 10^{-4}$ m, $\omega_{q1} = 0.7507 \times 10^9$; (c) V_K = 1500 volts, I_o = 6.571 ma, $b_d = 7.620 \times 10^{-4}$ m, $\omega_{q1} = 0.7792 \times 10^9$.

unchanged. The plasma wavelength varies with the total current, as indicated above.

d. Reducing the beam radius, while keeping the voltage and current constant, reduces the level of the maxima and increases the standing-wave ratio, thus further reducing the minima of the noise standing wave.

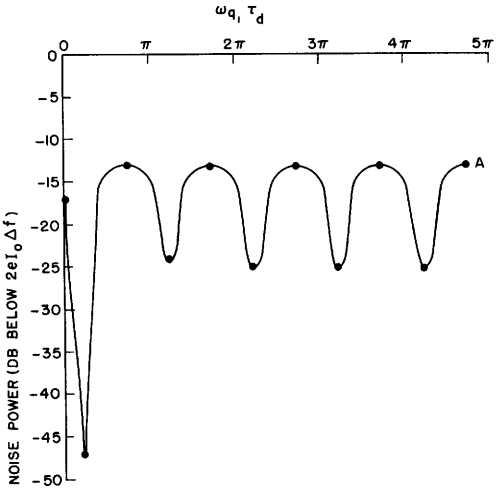

Fig. 5. Noise standing wave for gun A at V_K = 500 volts; V_K = 500 volts, I_o = 1.264 ma, $b_d = 7.620 \times 10^{-4}$ m, $\omega_{q1} = 0.6065 \times 10^9$, angle of convergence = 7.3°.

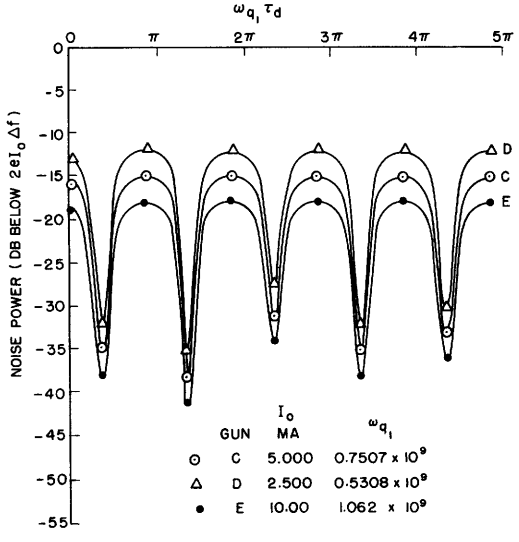

Fig. 6. Effect of perveance on the noise standing wave of parallel guns; V_K = 1250 volts, $b_d = 7.620 \times 10^{-4}$ m, angle of convergence = 0°.

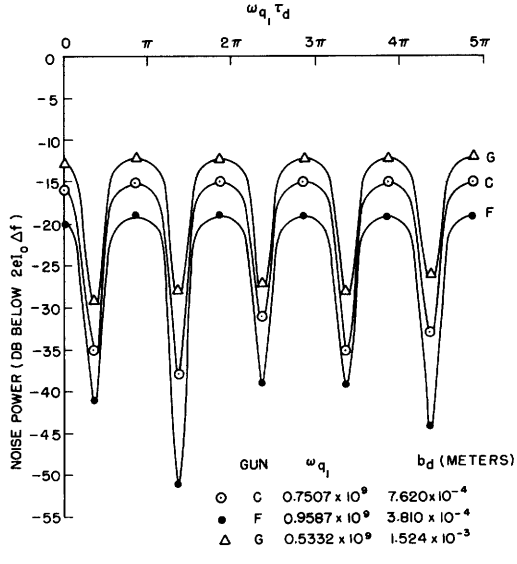

Fig. 7. Effect of beam radius on the noise standing wave of parallel guns; V_K = 1250 volts, I_o = 5.000 ma.

X. PARTITION NOISE

The foregoing analysis shows that the presence of the higher modes results in a noise standing wave in the drift space with a finite standing-wave ratio. It will be shown that this analysis also predicts a behavior of partition noise which is at least qualitatively similar to that observed experimentally, but whose mechanism is completely different from that of the usual theories based on compensating pulses or on the random interception of electrons by an electrode (4).

We wish to consider the problem illustrated in Fig. 8, in which a portion of the beam in the drift space is intercepted by an aperture whose center coincides with the axis of the beam and whose radius is smaller than the beam radius.

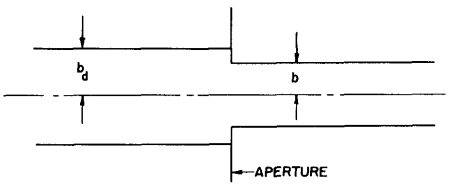

Fig. 8. Intercepting aperture in the drift space.

In view of the assumption of infinite magnetic field, all transverse motion of the electrons is inhibited; there is therefore no random interception of electrons by the aperture.

The noise in the beam to the left of the aperture may be calculated by the method presented above. We now wish to calculate the noise in that portion of the beam that passes through the intercepting aperture. To accomplish this, each of the modes in the beam to the left of the aperture must be expanded in an infinite series of the modes of the beam to the right of the aperture in such a manner that v and j are continuous across the plane of the aperture. These new modes have a different transverse dependence from that of the original modes; further, there are no simple orthogonality relationships. Therefore, this calculation would be quite tedious to carry out. But if we are interested only in the noise immediately behind the intercepting aperture, the calculation may be carried out in terms of the original modes without performing this expansion. Such a situation is approximately realized by the experiment described in reference 22, in which part of the beam current is intercepted in front of the noise-measuring-cavity gap.

To calculate the noise just beyond the aperture, it is necessary to average the current density of the different modes at the plane of the aperture only over a circle of radius b, instead of b_d. Therefore, the desired formula for the noise power as a function of the radius of the aperture b may be obtained by replacing b_d by b in Eqs. 85 and 92.

It can be seen that the convergence of these infinite series is made slower as b decreases; satisfactory results cannot be obtained with only the four terms of the series evaluated in these calculations. However, it is possible to see qualitatively what the behavior of partition noise will be.

The variation of the contribution of the n^{th} mode to the total noise power with b at

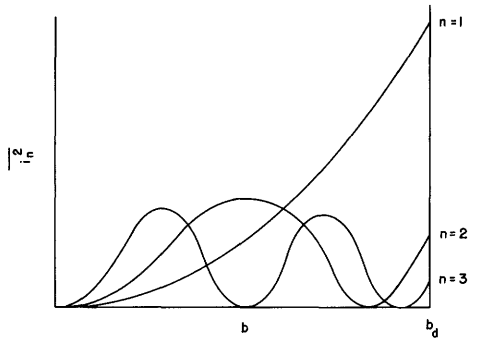

Fig. 9. Contributions to the noise power of the first three modes as functions of beam radius.

a fixed point along the beam is given by the expression

$$b^2 J_1^2(T_{nd}b)$$

whose general behavior is shown in Fig. 9 for the first three modes.

The amplitudes of the different modes vary with distance along the beam, the amplitude of each mode varying periodically with its proper plasma wavelength. Therefore, the amplitudes of the curves in Fig. 9 have no special significance and are intended to indicate only the proper radial variation.

We see that the contribution of the lowest mode to the noise power decreases monotonically to zero as b decreases from b_d to zero; the higher modes, however, have a very different behavior. For example, the contribution of the second mode decreases to zero for a value of b slightly smaller than b_d, then increases to a value very much greater than its initial value at $b = b_d$, and finally decreases to zero as b approaches zero. The other modes behave in an analogous manner. As shown in Fig. 9, the contribution of the n^{th} mode goes to zero for n - 1 values of the aperture radius and between these zeros attains values much higher than its initial value at $b = b_d$.

Let us now examine the behavior of partition noise at a minimum and at a maximum of the noise standing wave pattern. At a minimum the amplitude of the first mode is zero; the principal contribution to the noise power comes from the second and higher modes. Therefore, for values of b in the neighborhood of $(1/2)\, b_d$ the noise power will be many decibels greater than its value for zero partition current. This is in at least qualitative agreement with the behavior observed experimentally (22).

At a maximum of the standing-wave pattern the only significant contribution to the noise power comes from the first mode when there is no partition current. As b decreases from b_d, the contribution from the first mode decreases, while that from the second and higher modes increases; thus, it might be expected that the total noise power does not vary greatly for moderate amounts of partition current, a fact that is observed experimentally.

Although, as mentioned above, four terms of the series are not sufficient for obtaining an accurate calculation of the behavior of partition noise, the neglect of the higher terms will make the calculated results too small. Using only these four terms, the partition noise was calculated at the second minimum of the standing-wave pattern for gun A at 1250 volts. It was found that for the value of b that caused the contribution of the second mode to be equal to zero the total noise power was still greater than it was for zero partition current. This tends to suggest that the partition noise calculated in this manner does rise monotonically with partition current at a minimum of the standing-wave pattern if all the higher modes are taken into consideration and does not initially decrease, as might be inferred by considering only the first four modes. Experimental observations indicate that this must be the case (22).

XI. DISCUSSION

The effect of the higher modes of a beam confined by an infinite magnetic field on the noise standing wave in the drift space has been considered. The infinite magnetic field model has been chosen because it offers the simplest analysis. An approximate solution, using the method of Parzen, has been found for the sinusoidal modes of the beam in the gun region and these have been matched to the Ramo modes in the drift space. The input boundary conditions at the cathode have been specified by assuming that the Rack velocity modulation is statistically independent for each elementary area of the cathode, and these boundary conditions have been matched by the proper combination of the modes of the beam. Thus, the transverse variations of the noise current and velocity modulation are taken into account.

The excitation of the higher modes was shown to lead to a standing-wave ratio of noise current as low as 10 db (measured by an ideal cavity), with the different minima having different levels. In addition, the higher modes result in a type of partition noise which appears similar to that observed experimentally but has a different physical basis from that usually discussed in connection with partition noise.

Even the idealized infinite magnetic field model can be solved only in an approximate manner, by means of the WKB method. In order to evaluate the solutions, extensive numerical calculations are required. The approximations in the solution fail for guns that are too highly convergent or divergent.

In applying these results to actual situations we would expect to find good agreement for a parallel-beam gun confined by a strong magnetic field. For converging-beam guns that are similarly confined by a converging magnetic field in the gun and a uniform longitudinal field in the drift space (not a usual situation), the theory, because of the mathematical difficulties discussed above, will be less reliable if the gun is highly converging or diverging. Perhaps a more careful analysis can improve this situation. Finally, the application of these results to the converging-beam gun in zero magnetic field followed by a drift space with a uniform longitudinal field – which under ideal conditions should produce Brillouin flow but in practice falls short of this – is the least certain because of the use of the infinite magnetic field model. Here, a more rigorous analysis appears quite difficult even for ideal Brillouin flow.

In all of these cases, the gradual transition from the gun region to the drift space associated with the fringing fields near the anode aperture will cause a further departure from the analysis, which assumes an abrupt transition at the anode. This error will be more serious as the gun becomes more strongly convergent. If the effect of this aperture could be taken into account in the analysis, the mathematical difficulties associated with the too rapid variations in the beam parameters for converging beam guns would probably be eliminated.

Finally, we wish to compare the present analysis with an analysis given by C. F. Quate (23). He analyzed the propagation of space-charge waves in a spherically

symmetrical, space-charge-limited electron flow, and applied this analysis to the noise behavior of converging and diverging beam guns. This analysis differs from the present one in that it considers only the spherically symmetrical mode of a complete spherical flow; thus, the velocity and current density modulation are independent of the transverse coordinates.

Since it considers only the lowest mode, Quate's analysis yields an infinite standing-wave ratio in the drift space. It predicts that the level of the maxima of the noise standing wave should decrease as the gun is made more divergent. In contrast, the present analysis shows that the level of the maxima is smaller for a convergent gun than for a parallel gun.

The mathematical difficulties in the present analysis near the anode for converging guns may account for part of this discrepancy. However, the two analyses do differ in a rather fundamental way: in Quate's analysis the noise modulation is constant across the beam; in this analysis the modulation for the lowest mode, which yields the only significant contribution at the maxima, varies appreciably over the beam cross section in the gun, going to zero at the edge of the cathode. This analysis should become identical with Quate's if T_n is made identically equal to zero instead of being determined by Eq. 100. At any rate, it would be desirable to reconcile the differences in the behavior of the maxima in these two analyses.

In spite of various difficulties, the analysis presented in this report is suggestive of the part the higher modes play in the noise phenomena of an electron beam. For a confined parallel electron flow, the calculations would appear to merit some confidence.

XII. CONCLUSIONS

Experimental observations (22) on the noise standing wave pattern of an electron beam produced by a shielded Pierce gun showed an appreciable variation in the levels of the minima, thus suggesting the presence of more than one mode. The present analysis was undertaken in an attempt to evaluate the effect of the higher modes on the noise modulation of the beam. A simple model, in which confined flow was assumed in both the gun and in the drift space, was assumed in order to simplify the calculations. While the focusing conditions for a shielded gun followed by a drift space with a uniform magnetic field are quite different from those of the mathematical model, it was hoped that these calculations would give at least some qualitative ideas about the effects produced by the higher modes of the beam.

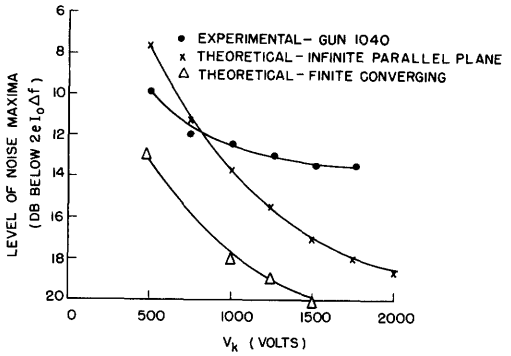

Fig. 10. Level of noise maxima vs. voltage for gun 1040.

The parameters of gun A used in these calculations were chosen to agree approximately with those of gun 1040 used in the experiments of reference 22 to facilitate some comparisons between experiment and theory. Figure 10 shows a plot of the level of the maxima of the noise current vs. voltage for gun 1040 together with two theoretical curves, one calculated by using the conventional infinite parallel plane analysis, the other by using the analysis of this report. Although neither agrees with the experimental curve very well, the infinite parallel plane analysis is somewhat better than the more elaborate theory given here, which yields values between 3 db and 6 db below the experimental values.

The experimental standing-wave ratios for gun 1040 (see ref. 22) at low magnetic fields usually varied between 8 db and 10 db. The calculations for gun A yielded standing-wave ratios between 10 db and 13 db except for the first minimum, which varied between 34 db and 39 db below the maxima. In no instance was the experimental level of the first minimum observed to be a great deal lower than the other minima.

It also is interesting to compare the space phase of the standing-wave pattern with the theoretical values. This is specified by the distance from the anode to the first minimum measured in plasma degrees. The measured distance on gun 1040 was 82°. The infinite parallel plane theory yields a value of 55°, while the theory of this report yields a value of 33°. While neither calculation seems particularly good, the infinite parallel plane theory again seems somewhat better.

It would be interesting to make similar comparisons for a parallel confined gun. While no extensive measurements are available, C. E. Muehe (24) has obtained some results for a gun quite similar to gun D of Section IX. This gun has a beam radius of

7.1×10^{-4} m. At a beam voltage of 1000 volts and a beam current of 1.5 ma, the maxima of the noise standing wave were 14 db below shot noise, and the standing-wave ratio was about 13 db. At a beam voltage and current of 1250 volts and 2.5 ma, respectively, the maxima of gun D are 12 db below shot noise and the standing-wave ratio varies between 16 db and 23 db. The infinite parallel plane theory places the level of the maxima 14 db below shot noise for these conditions. Further, Muehe found the distance from the anode to the first minimum to be 69°. The present theory predicts a value of 62°; the infinite parallel plane theory yields 35°.

In contrast with the converging gun, the theory presented here appears to be somewhat more accurate for a confined parallel gun. The difficulties in the analysis near the anode may be responsible for some of the discrepancies in the calculations for the converging gun; differences between the behavior of the infinite magnetic field model and the physical situation may also play an important part. Considering the effect of the aperture in the anode should make the results for the converging gun closer to those for the parallel gun by removing the effect of the singularity at the focus of the converging flow.

The electron trajectories for the converging-beam gun are fairly complex in practice, and an accurate analysis seems almost out of reach. By comparison, the flow conditions in the parallel-beam gun confined by a strong magnetic field are considerably simpler. A detailed experimental study of the noise behavior of confined parallel-beam guns would appear quite useful. A comparison of both the standing-wave pattern and the behavior of partition noise with the results of the theory would help in evaluating the basic ideas used in the present analysis.

ACKNOWLEDGMENT

The author wishes to thank Professor L. J. Chu for his many helpful suggestions during his supervision of this work. He is indebted to Mr. L. D. Smullin for his continued advice and encouragement during the course of this investigation, to Professor S. J. Mason for his interest in the work, and to Professor H. A. Haus and Mr. C. E. Muehe for many helpful discussions. He also wishes to thank Mrs. Hannah R. Wasserman for performing the many tedious calculations the results of which are presented in this report.

APPENDIX A

THE WENTZEL-KRAMERS-BRILLOUIN METHOD (17, 18)

Certain features of the WKB method will be reviewed in this section for easy reference. We wish to solve approximately the following type of differential equation:

$$\frac{d^2y}{dx^2} + k^2(x)y = 0 \tag{A-1}$$

Let

$$y = \exp\left[j \int^x u\, dx\right] \tag{A-2}$$

Then u satisfies the differential equation

$$u^2 = k^2 + j\frac{du}{dx} = k^2 + ju' \tag{A-3}$$

where the prime denotes differentiation. This equation is solved by successive approximations in which u_0, u_1, and so forth, are successively better approximations to u. Assume as a first approximation that

$$u_0 = k \qquad u_0' = k' \tag{A-4}$$

Substituting Eq. A-4 into the right-hand side of Eq. A-3 will give us the next approximation for u. Using the binomial expansion,

$$u_1 = k + \frac{jk'}{2k} \tag{A-5}$$

This gives the usual WKB solution, which will be a good approximation if the following inequality, which permits the retention of only the first two terms of the binomial expansion, is satisfied:

$$k' \ll k^2 \tag{A-6}$$

Then, substituting Eq. A-5 into Eq. A-2, we obtain, as the final result,

$$y \approx \frac{\exp\left[\pm j\int^x k\, dx\right]}{k^{1/2}} \tag{A-7}$$

where the plus and minus signs in the exponent give the two solutions to the original differential equation.

This solution fails near the zeros and poles of k^2. It is, however, sometimes possible to determine a solution which is exact near the zero or pole and approaches

the WKB solution, given in Eq. A-7, far from this point. For example, if

$$k^2 \to c\, x^n \quad \text{as} \quad x \to 0 \tag{A-8}$$

an appropriate solution is

$$y \approx \left(\frac{\int_0^x k\, dx}{k} \right)^{1/2} J_{\pm\frac{1}{n+2}} \left(\int_0^x k\, dx \right) \tag{A-9}$$

where J denotes a Bessel function of the first kind. This solution is exact near x = 0; for large x, it approaches the solution given by Eq. A-7.

This discussion is applicable only if k^2 remains positive; the expressions for negative k^2 are easily derived. Let us write the differential equation in the following form:

$$\frac{d^2y}{dx^2} - \kappa^2(x)y = 0 \tag{A-10}$$

κ^2 is now assumed to remain positive. The WKB solution becomes

$$y \approx \frac{\exp\left(\pm \int^x \kappa\, dx \right)}{\kappa^{1/2}} \tag{A-11}$$

This solution is valid away from the poles and zeros of κ^2. If

$$\kappa^2 \to c\, x^n \quad \text{as} \quad x \to 0, \tag{A-12}$$

an appropriate solution analogous to that of Eq. A-9 is

$$y \approx \left(\frac{\int_0^x \kappa\, dx}{\kappa} \right)^{1/2} I_{\pm\frac{1}{n+2}} \left(\int_0^x \kappa\, dx \right) \tag{A-13}$$

where I denotes a modified Bessel function of the first kind.

APPENDIX B

SERIES REPRESENTATIONS FOR CERTAIN SPHERICAL FUNCTIONS RELATED TO THOSE OF LANGMUIR AND BLODGETT (19)

Langmuir and Blodgett have given the solution for the potential distribution in a spherically-symmetric, space-charge-limited electron flow in terms of a parameter α. This parameter satisfies the following nonlinear differential equation:

$$3\alpha \frac{d^2\alpha}{d\gamma^2} + \left(\frac{d\alpha}{d\gamma}\right)^2 + 3\alpha \frac{d\alpha}{d\gamma} - 1 = 0 \tag{B-1}$$

$$\gamma = -\ln \mu \qquad \mu = \frac{R_k}{R} \tag{B-2}$$

α is given in terms of an infinite series in γ as follows:

$$\alpha = \gamma - 0.3\gamma^2 + 0.075\gamma^3 - 0.0143182\gamma^4 + 0.0021609\gamma^5 - 0.00026791\gamma^6 + 0.000028444\gamma^7 - \ldots \tag{B-3}$$

The first three coefficients of this series are exact; the remainder have been rounded off.

As will be seen in Appendix C, the function $f(\mu)$ is directly related to the potential, where f is defined as

$$f = |\alpha|^{4/3} \tag{B-4}$$

Transforming Eq. B-1 so that f becomes the dependent variable and μ the independent variable, we obtain the differential equation

$$\mu^2 \frac{d^2 f}{d\mu^2} = \frac{4}{9} f^{-1/2} \tag{B-5}$$

This equation is useful because later we shall wish to compute the first and second derivatives of f with respect to μ. Equation B-5 permits us to compute the second derivative directly once the value of f is known.

The utility of the various functions given below will be shown in Appendix C. The various series were obtained from the series given in Eq. B-3 by means of the binomial expansion.

$$f = |\gamma|^{4/3} (1 - 0.4\gamma + 0.12\gamma^2 - 0.027757\gamma^3 + 0.0052069\gamma^4 - 0.0008217\gamma^5 + 0.00011200\gamma^6 - \ldots) \tag{B-6}$$

$$\frac{df}{d\mu} = \pm 1.3333 \frac{|\gamma|^{1/3}}{\mu} (1 - 0.7\gamma + 0.3\gamma^2 - 0.090210\gamma^3 + 0.020828\gamma^4 - 0.003903\gamma^5 + 0.00061600\gamma^6 - \ldots) \tag{B-7}$$

The plus sign applies to the converging case, the minus sign to the diverging case.

$$f^{1/2} = |\gamma|^{2/3} (1 - 0.2\gamma + 0.04\gamma^2 - 0.005879\gamma^3 + 0.0006277\gamma^4 - 0.00005016\gamma^5 + 0.00000359\gamma^6 - \ldots) \quad \text{(B-8)}$$

$$f^{-1/2} = |\gamma|^{-2/3} (1 + 0.2\gamma - 0\gamma^2 - 0.002121\gamma^3 + 0.000124\gamma^4 + 0.0000342\gamma^5 - 0.0000041\gamma^6 - \ldots) \quad \text{(B-9)}$$

$$k = \pm\frac{1}{3}\int_1^{\mu} \frac{d\mu}{\mu^2 f^{1/2}(\mu)} = \mp\frac{1}{3}\int_0^{\gamma} e^{+\gamma} f^{-1/2}\, d\gamma$$

$$= |\gamma|^{1/3} (1 + 0.3\gamma + 0.1\gamma^2 + 0.026455\gamma^3 + 0.0056156\gamma^4 + 0.0009852\gamma^5 + 0.00014705\gamma^6 + \ldots) \quad \text{(B-10)}$$

(The top signs apply to the converging case, the bottom signs to the diverging case.)

$$h = \frac{1}{\mu f^{1/2}} \quad \text{(B-11)}$$

$$j = \frac{4}{9}\frac{\mu^2}{f^{1/2}} \quad \text{(B-12)}$$

$$i = 2\mu^3 \frac{df}{d\mu} + j \quad \text{(B-13)}$$

$$m = \frac{\mu^2}{f^{1/2}} \frac{df}{d\mu} \quad \text{(B-14)}$$

APPENDIX C

PARAMETERS OF SPHERICAL CONVERGING AND DIVERGING GUNS

The following formulas give the various parameters needed in the calculations for spherical guns. The functions involved in these formulas, which were defined in Appendix B, are tabulated in Appendix E.

$$K_n^2 = \left(\frac{9\eta}{4(2)^{1/2}\,\epsilon}\right)^{2/3}\left(\frac{J_{ok}}{R_k}\right)^{2/3}\left[i(\mu) - j(\mu)\,\frac{1}{1+\left(T_n^2/\gamma_o^2\right)}\right]$$

$$= 9.998 \times 10^{14}\left(\frac{J_{ok}}{R_k}\right)^{2/3}\left[i(\mu) - j(\mu)\,\frac{1}{1+\left(T_n^2/\gamma_o^2\right)}\right] \qquad \text{(C-1)}$$

$$\text{As} \quad \mu \to 1,\ K_n^2 \to 2\,\frac{\eta}{\epsilon}\left(\frac{J_{ok}}{R_k}\right)\tau = 3.972 \times 10^{22}\,\frac{J_{ok}}{R_k}\,\tau \qquad \text{(C-2)}$$

$$\tau = \left(\frac{6\epsilon}{\eta}\right)^{1/3}\left(\frac{R_k}{J_{ok}}\right)^{1/3} k(\mu) = 6.710 \times 10^{-8}\left(\frac{R_k}{J_{ok}}\right)^{1/3} k(\mu) \qquad \text{(C-3)}$$

$$b = \frac{b_k}{\mu} \qquad \text{(C-4)}$$

$$J_o = \mu^2 J_{ok} \qquad \text{(C-5)}$$

$$\gamma_o b = \left(\frac{2\epsilon}{9\eta}\right)^{1/3}\frac{\omega b_k}{\left(R_k^2 J_{ok}\right)^{1/3}} h(\mu) = 2.237 \times 10^{-8}\,\frac{\omega b_k}{\left(R_k^2 J_{ok}\right)^{1/3}} h(\mu) \qquad \text{(C-6)}$$

$$V_o = \left[\frac{9}{4\epsilon(2\eta)^{1/2}}\right]^{2/3}\left(R_k^2 J_{ok}\right)^{2/3} f(\mu) = 5.685 \times 10^3\left(R_k^2 J_{ok}\right)^{2/3} f(\mu) \qquad \text{(C-7)}$$

$$v_o = \left(\frac{9\eta}{2\epsilon}\right)^{1/3}\left(R_k^2 J_{ok}\right)^{1/3} f^{1/2}(\mu) = 4.471 \times 10^7\left(R_k^2 J_{ok}\right)^{1/3} f^{1/2}(\mu) \qquad \text{(C-8)}$$

$$\frac{v_o'}{v_o} = \frac{1}{v_o}\frac{dv_o}{d\tau} = \frac{dv_o}{dz} = \frac{1}{2}\left(\frac{9\eta}{2\epsilon}\right)^{1/3}\left(\frac{J_{ok}}{R_k}\right)^{1/3} m(\mu)$$

$$= 2.235 \times 10^7\left(\frac{J_{ok}}{R_k}\right)^{1/3} m(\mu) \qquad \text{(C-9)}$$

APPENDIX D

TABLES OF BESSEL FUNCTIONS

The combinations of Bessel functions given below are of use in solving the transcendental matching equation, Eq. 100, for T_n, the radial wave number.

Linear interpolation is not satisfactory in all portions of these tables.

x	$x\frac{K_1(x)}{K_0(x)}$	x	$x\frac{K_1(x)}{K_0(x)}$
0.	0.00000	5.6	6.08084
0.2	0.54498	5.8	6.28142
0.4	0.78396	6.0	6.48196
0.6	1.00537	6.5	6.98318
0.8	1.21947	7.0	7.48425
1.0	1.42963	7.5	7.98519
1.2	1.63735	8.0	8.48602
1.4	1.84347	8.5	8.98677
1.6	2.04844	9.0	9.48744
1.8	2.25258	9.5	9.98804
2.0	2.45607	10.0	10.48859
2.2	2.65907	11.0	11.48955
2.4	2.86168	12.0	12.49035
2.6	3.063966	13.0	13.49105
2.8	3.26599	14.0	14.49165
3.0	3.46779	15.0	15.49217
3.2	3.66941	16.0	16.49263
3.4	3.87087	17.0	17.49304
3.6	4.07219	18.0	18.49341
3.8	4.27340	19.0	19.49374
4.0	4.47450	20.0	20.49404
4.2	4.67552	25.0	25.4952
4.4	4.87646	30.0	30.4959
4.6	5.07732	35.0	35.4965
4.8	5.27813	40.0	40.4969
5.0	5.47888	45.0	45.4973
5.2	5.67957	50.0	50.4975
5.4	5.88023		

As $x \to \infty$, $x\frac{K_1(x)}{K_0(x)} \to x + 0.5$

$x_n\frac{J_1(x_n)}{J_0(x_n)}$	x_1	x_2	x_3	x_4
0.	0.000	3.832	7.016	10.174
0.1	0.442	3.858	7.030	10.183
0.2	0.617	3.884	7.044	10.193
0.3	0.746	3.909	7.058	10.203
0.4	0.852	3.934	7.072	10.213
0.5	0.941	3.959	7.086	10.222
0.6	1.018	3.984	7.100	10.232
0.7	1.087	4.009	7.114	10.242
0.8	1.150	4.032	7.128	10.252
0.9	1.205	4.056	7.142	10.261
1.0	1.256	4.079	7.156	10.271
1.1	1.303	4.102	7.169	10.281
1.2	1.345	4.125	7.183	10.290
1.3	1.385	4.147	7.197	10.300
1.4	1.423	4.169	7.210	10.309
1.5	1.457	4.190	7.223	10.319
1.6	1.489	4.211	7.237	10.328
1.7	1.519	4.232	7.250	10.338
1.8	1.547	4.252	7.263	10.347
1.9	1.574	4.272	7.276	10.357
2.0	1.599	4.291	7.288	10.366
3.0	1.789	4.463	7.410	10.457
4.0	1.908	4.602	7.520	10.542
5.0	1.990	4.713	7.618	10.622
6.0	2.049	4.803	7.704	10.696
7.0	2.094	4.877	7.780	10.765
8.0	2.129	4.938	7.846	10.827
9.0	2.156	4.990	7.905	10.884
10.0	2.179	5.033	7.957	10.936
15.0	2.251	5.117	8.142	11.137
20.0	2.288	5.257	8.253	11.268
25.0	2.311	5.307	8.326	11.357
30.0	2.326	5.341	8.377	11.422
35.0	2.337	5.366	8.415	11.471
40.0	2.346	5.385	8.443	11.508
45.0	2.352	5.399	8.466	11.538
50.0	2.357	5.411	8.484	11.562
∞	2.405	5.520	8.654	11.792

As $x\frac{J_1(x)}{J_0(x)} \to \infty$, $x_n \to \frac{x_{n\infty}}{1 + \frac{1}{x\frac{J_1(x)}{J_0(x)}}}$

APPENDIX E

TABLES OF SPHERICAL FUNCTIONS

Converging Guns

μ	$1/\mu$	$i(\mu)$	$j(\mu)$	$i(\mu) - j(\mu)$	$k(\mu)$	$h(\mu)$	$m(\mu)$	$f(\mu)$	$f^{1/2}(\mu)$	$df/d\mu$
1.0	1.00000	∞	∞	0.	0.	∞	∞	0.	0.	0.
1.000001	1.00000	4444.4	4444.4	0.026667	0.010000	10000.	133.33	0.1×10^{-7}	0.1×10^{-3}	0.013333
1.00001	0.99999	957.60	957.54	0.057451	0.021544	2154.5	61.887	0.21544×10^{-6}	0.46415×10^{-3}	0.028725
1.0001	0.99990	206.46	206.34	0.12381	0.046414	464.12	28.731	0.46415×10^{-5}	0.0021544	0.061885
1.0005	0.99960	70.838	70.626	0.21192	0.079352	158.67	16.813	0.39680×10^{-4}	0.0062992	0.10580
1.001	0.99900	44.806	44.539	0.26734	0.099953	99.913	13.355	0.99973×10^{-4}	0.0099987	0.13327
1.005	0.99502	15.824	15.362	0.46181	0.17060	34.052	7.8623	0.85387×10^{-3}	0.029221	0.22747
1.01	0.99010	10.3698	9.7806	0.58919	0.21445	21.359	6.2922	0.0021488	0.046355	0.28593
1.02	0.98039	7.0534	6.2923	0.76109	0.26895	13.341	5.0769	0.0054004	0.073487	0.35860
1.03	0.97087	5.7959	4.9029	0.89302	0.30647	10.095	4.5079	0.0092484	0.096169	0.40863
1.04	0.96154	5.1389	4.1316	1.0073	0.33581	8.2642	4.1623	0.013537	0.11635	0.44775
1.05	0.95238	4.7457	3.6339	1.1118	0.36015	7.0630	3.9263	0.018181	0.13484	0.48020
1.06	0.94340	4.4941	3.2839	1.2102	0.38103	6.2037	3.7538	0.023126	0.15207	0.50804
1.07	0.93458	4.3278	3.0231	1.3047	0.39939	5.5524	3.6222	0.028331	0.16832	0.53252
1.08	0.92593	4.2178	2.8211	1.3967	0.41580	5.0388	3.5189	0.033768	0.18376	0.55439
1.09	0.91743	4.1469	2.6599	1.4870	0.43061	4.6213	3.4362	0.039412	0.19852	0.57415
1.10	0.90909	4.1046	2.5282	1.5764	0.44413	4.2738	3.3686	0.045245	0.21271	0.59218
1.15	0.86957	4.1420	2.1216	2.0204	0.49817	3.1387	3.1707	0.076759	0.27705	0.66422
1.20	0.83333	4.3962	1.9179	2.4783	0.53782	2.4972	3.0945	0.11135	0.33370	0.71710
1.25	0.80000	4.7658	1.8034	2.9624	0.56879	2.0775	3.0773	0.14828	0.38507	0.75838
1.30	0.76923	5.2162	1.7367	3.4795	0.59391	1.7786	3.0942	0.18706	0.43250	0.79187
1.35	0.74074	5.7325	1.6987	4.0338	0.61482	1.5535	3.1331	0.22737	0.47683	0.81974
1.40	0.71429	6.3082	1.6797	4.6285	0.63254	1.3773	3.1874	0.26897	0.51862	0.84339
1.45	0.68956	6.9402	1.6739	5.2663	0.64780	1.2354	3.2529	0.31165	0.55826	0.86372
1.50	0.66667	7.6275	1.6777	5.9498	0.66109	1.1184	3.3272	0.35530	0.59607	0.88145
1.6	0.62500	9.1668	1.7057	7.4611	0.68309	0.93698	3.4954	0.44495	0.66704	0.91078
1.7	0.58824	10.9317	1.7524	9.1793	0.70064	0.80253	3.6833	0.53726	0.73298	0.93418
1.8	0.55556	12.930	1.8118	11.118	0.71491	0.69901	3.8859	0.63167	0.79478	0.95321
1.9	0.52632	15.173	1.8807	13.292	0.72674	0.61695	4.1004	0.72778	0.85310	0.96898
2.0	0.50000	17.673	1.9568	15.716	0.73671	0.55035	4.3248	0.82538	0.90851	0.98228
2.1	0.47619	20.443	2.0388	18.404	0.74521	0.49533	4.5580	0.92420	0.96135	0.99361
2.2	0.45455	23.494	2.1258	21.368	0.75252	0.44920	4.7993	1.0240	1.0119	1.0034
2.3	0.43478	26.838	2.2168	24.621	0.75889	0.40994	5.0466	1.1248	1.0606	1.0118
2.4	0.41667	30.494	2.3117	28.182	0.76446	0.37626	5.3018	1.2264	1.1074	1.0193
2.5	0.40000	34.466	2.4100	32.056	0.76938	0.34704	5.5624	1.3286	1.1526	1.0258

Diverging Guns

μ	$1/\mu$	$i(\mu)$	$j(\mu)$	$i(\mu) - j(\mu)$	$k(\mu)$	$h(\mu)$	$m(\mu)$	$f(\mu)$	$f^{1/2}(\mu)$	$df/d\mu$
1.00000	1.00000	∞	∞	0.	0.	∞	$-\infty$	0.	0.	0.
0.99999	1.00001	957.47	957.53	-0.057448	0.021544	2154.9	-61.886	0.21544×10^{-6}	0.00046415	-0.028725
0.99990	1.00010	206.13	206.25	-0.123747	0.046418	464.19	-28.721	0.46417×10^{-5}	0.0021545	-0.061892
0.99950	1.00050	70.264	70.475	-0.21139	0.079389	158.807	-16.7848	0.39691×10^{-4}	0.0063001	-0.105852
0.99900	1.00100	44.084	44.350	-0.26599	0.100047	100.087	-13.3112	0.100027×10^{-3}	0.0100013	-0.133396
0.99502	1.00500	14.6290	15.0787	-0.44965	0.171167	34.439	-7.7428	0.85156×10^{-3}	0.029182	-0.22822
0.99010	1.01000	8.8789	9.4372	-0.55835	0.21572	21.877	-6.1075	0.0021314	0.046167	-0.28763
0.98039	1.02000	5.1750	5.8589	-0.68393	0.27218	13.9895	-4.7839	0.0053162	0.072912	-0.36290
0.97087	1.03000	3.6463	4.4076	-0.76133	0.31198	10.8366	-4.1252	0.0090341	0.095048	-0.41597
0.96154	1.04000	2.7727	3.5877	-0.81504	0.34380	9.0802	-3.7003	0.0131182	0.114535	-0.45840
0.95238	1.05000	2.1943	3.0486	-0.85429	0.37085	7.9405	-3.3917	0.0174859	0.132234	-0.49447
0.94340	1.06000	1.7791	2.6626	-0.88353	0.39459	7.1350	-3.1520	0.022071	0.148563	-0.52613
0.93458	1.07000	1.4642	2.3696	-0.90542	0.41594	6.5314	-2.9569	0.026838	0.163822	-0.55459
0.92593	1.08000	1.2167	2.1385	-0.92179	0.43543	6.0612	-2.7935	0.031749	0.178182	-0.58058
0.91743	1.09000	1.01661	1.95038	-0.93377	0.45346	5.6830	-2.6533	0.036787	0.191799	-0.60463
0.90909	1.10000	0.85174	1.79393	-0.94219	0.47028	5.3724	-2.5309	0.041924	0.20475	-0.62703
0.86957	1.15000	0.33287	1.28280	-0.94993	0.54176	4.3896	-2.0849	0.068636	0.26198	-0.72235
0.83333	1.20000	0.06889	0.99487	-0.92598	0.60002	3.8681	-1.79089	0.096242	0.31023	-0.80005
0.80000	1.25000	-0.08027	0.80767	-0.88794	0.65035	3.5493	-1.57579	0.124031	0.35218	-0.86713
0.76923	1.30000	-0.16858	0.67534	-0.84392	0.69530	3.3384	-1.40867	0.151643	0.38941	-0.92706
0.74074	1.35000	-0.22138	0.57667	-0.79805	0.76633	3.1923	-1.27383	0.178838	0.42289	-0.98176
0.71429	1.40000	-0.25230	0.50025	-0.75255	0.77437	3.0885	-1.16213	0.20547	0.45329	-1.03248
0.68966	1.45000	-0.26918	0.43936	-0.70854	0.81003	3.0137	-1.06768	0.23149	0.48113	-1.08003
0.66667	1.50000	-0.27690	0.38978	-0.66668	0.84376	2.9599	-0.98664	0.25683	0.50678	-1.12501
0.62500	1.60000	-0.27615	0.31413	-0.59028	0.90667	2.8950	-0.85443	0.30544	0.55267	-1.20890
0.58824	1.70000	-0.26426	0.25947	-0.52373	0.96484	2.8682	-0.75106	0.35130	0.59271	-1.28648
0.55556	1.80000	-0.24768	0.21839	-0.46607	1.01944	2.8657	-0.66780	0.39453	0.62812	-1.35901
0.52632	1.90000	-0.22986	0.186609	-0.41647	1.07119	2.8799	-0.59969	0.43527	0.65975	-1.42826
0.50000	2.00000	-0.21211	0.161435	-0.37355	1.12065	2.9058	-0.54273	0.47372	0.68827	-1.49419
0.47619	2.10000	-0.19524	0.141120	-0.33636	1.16817	2.9405	-0.49455	0.51003	0.71416	-1.55753
0.45455	2.20000	-0.17960	0.124461	-0.30406	1.21408	2.9817	-0.45331	0.54440	0.73783	-1.61874
0.43478	2.30000	-0.16524	0.110606	-0.27585	1.25861	3.0279	-0.41763	0.57698	0.75959	-1.67815
0.41667	2.40000	-0.15217	0.098967	-0.25114	1.30189	3.0782	-0.38653	0.60788	0.77967	-1.73586
0.40000	2.50000	-0.14032	0.089078	-0.22940	1.34414	3.1317	-0.35920	0.63729	0.79830	-1.79217

References

1. S. Ballentine, Shot-effect in high frequency circuits, J. Frank. Inst. 206, 159 (1928).
2. G. E. Duvall, The effects of transit angle on shot noise in vacuum tubes, Ph. D. Thesis, Department of Physics, M.I.T. (1948).
3. W. Schottky, Spontaneous current fluctuations in various conductors, Ann. Physik 57, 541 (1918).
4. B. J. Thompson, D. O. North, and W. A. Harris, Fluctuations in space-charge-limited currents at moderately high frequencies, R.C.A. Review, Parts I-V; Vol. IV, Nos. 3,4; Vol. V., Nos. 1,2,3,4; Vol. VI, No. 1.
5. F. B. Llewellyn, Electron-Inertia Effects (Cambridge University Press, London, 1943).
6. S. Ramo, The electronic-wave theory of velocity-modulation tubes, Proc. I.R.E. 27, 757 (1939).
7. L. D. Smullin, Propagation of disturbances in accelerated electron streams: 1, One-dimensional accelerated streams, Technical Report 207, Research Laboratory of Electronics, M.I.T. (1951); J. Appl. Phys. 22, 1496 (1951).
8. J. R. Pierce, Traveling-Wave Tubes (D. Van Nostrand, Inc., New York, 1950).
9. A. J. Rack, Effect of space charge and transit time on the shot noise in diodes, Bell System Tech. J. 17, 592 (1938).
10. L. D. Smullin, Shot noise in beam type traveling-wave amplifiers, Technical Report 142, Research Laboratory of Electronics, M.I.T. (1949).
11. D. A. Watkins, Noise reduction in beam type amplifiers, Technical Report No. 31, Electronics Research Laboratory, Stanford University, Stanford, California (1951).
12. D. A. Watkins, Traveling-wave tube noise figure, Proc. I.R.E. 40, 65 (1952).
13. C. C. Cutler and C. F. Quate, Experimental verification of space charge and transit time reduction of noise in electron beams, Phys. Rev. 80, 875 (1950).
14. L. C. Peterson, Space-charge and transit-time effects on signal and noise in microwave tetrodes, Proc. I.R.E. 35, 1264 (1947).
15. L. T. Zitelli, Space-charge effects in gridless klystrons, Microwave Laboratory Report 149, Stanford University, Stanford, California (1951).
16. P. Parzen, The propagation of space-charge waves in a cylindrical electron beam of finite lateral extension, Technical Memorandum 422, Fed. Tel. Labs.; J. Appl. Phys. 23, 215 (1952).
17. P. M. Morse and H. Feshbach, Methods of Theoretical Physics (Technology Press, Cambridge, Massachusetts, 1946).
18. L. I. Schiff, Quantum Mechanics (McGraw-Hill Book Company, Inc., New York, 1949).
19. L. Langmuir and K. Blodgett, Currents limited by space charge between concentric spheres, Phys. Rev. 24, 49 (1924).
20. F. B. Hildebrand, Advanced Calculus for Engineers (Prentice-Hall, Inc., New York, 1949).
21. G. N. Watson, A Treatise on the Theory of Bessel Functions (Cambridge University Press, London, 1948).
22. H. E. Rowe, Shot noise in electron beams at microwave frequencies, D. Sc. Thesis, Department of Electrical Engineering, M.I.T. (1952).
23. C. F. Quate, The effect of diverging electron beams on noise space-charge waves, Bell Labs. Memorandum MM-52-150-11, April 28, 1952.
24. C. E. Muehe, Noise figure of traveling-wave tubes, M. Sc. Thesis, Department of Electrical Engineering, M.I.T. (1952).
25. H. A. Haus, unpublished work and Quarterly Progress Report, Research Laboratory of Electronics, M.I.T.: Oct. 15, 1951, Jan. 15, April 15, July 15, 1952.